DEVELOPMENT OF FLOOD FORECASTING SYSTEM FOR DELHI CITY

A DISSERTATION

SUBMITTED IN PARTIAL FULFILLMENT OF THE REQUIREMENTS

FOR THE AWARD OF THE DEGREE OF

MASTER OF TECHNOLOGY

IN

HYDRAULICS AND WATER RESOURCES ENGINEERING

Submitted by

VARUN AGGARWAL

Roll No. 2K20/HFE/07

Under the supervision of

Prof. T VIJAYA KUMAR

Professor, DTU

30/5/22

DEPARTMENT OF CIVIL ENGINEERING

DELHI TECHNOLOGICAL UNIVERISTY

(Formerly Delhi College of Engineering)

Bawana Road, Delhi – 110042

May, 2022

DELHI TECHNOLOGICAL UNIVERSITY

(Formerly Delhi College of Engineering)

Bawana Road, Delhi – 110042

CANDIDATE'S DECLERATION

I, Varun Aggarwal, Roll No. 2K20/HFE/07, student of M.Tech (Hydraulics and Water Resources), hereby declare that the project Dissertation "Development of Flood Forecasting System for Delhi City" is submitted by me to the Department of Civil Engineering, Delhi Technological University, Delhi in partial fulfilment of the requirements for the award of the degree of Master of Technology. The content of this thesis is original and not copied from any source without proper citation. This work has not previously formed the basis for award of any Degree, Diploma Associates, Fellowships or other similar title or recognition.

Varun

Place: Delhi

Date: 30-05-2022

VARUN AGGARWAL

2K20/HFE/07

DEPARTMENT OF CIVIL ENGINEERING

DELHI TECHNOLOGICAL UNIVERSIRTY

(Formerly Delhi College of Engineering)

Bawana Road, Delhi – 110042

CERTIFICATE

I hereby certify that the project Dissertation titled "Development of Flood Forecasting System for Delhi City" which is submitted by Varun Aggarwal, Roll No 2K20/HFE/07, Department of Civil Engineering, Delhi Technological University, Delhi in partial fulfilment of the requirement for the award of the degree of Master of Technology, is a record of the project work carried out by him under my supervision. To the best of my knowledge this work has not been submitted in part or full for any Degree or Diploma to this University or elsewhere.

Place: Delhi

Date: 30/5/22

Prof. T. VIJAYA KUMAR

SUPERVISOR

Professor

Department of Civil Engineering

Delhi Technological University

Bawana Road, Delhi - 110042

ABSTRACT

Floods annually affect a large population of Indian population during the monsoon months from June to September every year. Flooding leads to the disruption in the socio-economic conditions and causes enormous damage to infrastructure and agriculture. Without proper mechanism to predict the future conditions, it becomes very difficult for the authorities and the rescue teams to help relocate people to safer place and prevent loss of life and property. Also frequent and severe floods may affect the hydraulic structures, roads and nearby buildings as well. It may become very difficult for engineer to design structures based on future conditions. Therefore, accurate prediction of streamflow in rivers has become the need of the hour. For that accurate prediction of input data such as rainfall and potential evapotranspiration data is very much important. India has already worked over the ensemble prediction of rainfall data. The only challenge now lies in the ensemble prediction of streamflow data in different channels and at different gauge points. Once this mechanism gets established, then it would be very easy for a person to design future hydraulic projects and may select the factor of safety in the design appropriately. This may help in saving the project cost to a very great extent. Also it will help engineers to design the master plan of a particular city but checking of the extent of spread of the future city near the river banks and may also help in clearing of illegal encroachments along the river beds which may become frequently flooded in the future. In this project, I tried to prepare a flood forecasting system for a Yamuna Ghat gauge point in Delhi. For that I used the rainfall and potential evapotranspiration data for a period starting from 01-01-2001 and ending on 31-12-2011. Also I considered one-year warm-up period while calibrating the model. During this time the model may get some estimate of the initial condition and this may be beneficial for its future simulation. After obtaining the results, there was some discrepancy between the simulated streamflow and the observed streamflow. To improvise the results, there are two options, either to manually calibrate the model or use automatic calibration to perform a number of simulations and obtain model parameters which can give us the best results. Therefore, I used automatic calibration, plotted the resultant hydrograph and calculated various model indices to check for the accuracy of the results.

ACKNOWEDGEMENT

I am very thankful to vice chancellor of Delhi Technological University, Prof. Jai Prakash Saini and Prof. VK Minocha (Head of Department, Civil Engineering, DTU). I am grateful to Dr Manabendra Saharia, Assistant Professor, Department of Civil Engineering, Indian Institute of Technology, Delhi for helping me choose the project and Mr. Sai Kiran Kuntla, PhD scholar, Indian Institute of Technology, Delhi who helped me to overcome the obstacles and difficulties during the research work. I am very grateful to Prof. T. Vijaya Kumar who always motivated me and has supervised in all difficult times. He has always encouraged me to do better with his comments. He has always pointed my mistakes so I can be better.

I would like to thank all the faculties and professors of Civil Engineering Department, Delhi Technological University, for their kind gratitude. I also want to thank my friends and family who helped me overcome every obstacle and to be better.

Varun

Place: Delhi

Date: 30-05-2022

VARUN AGGARWAL

2K20/HFE/07

CONTENTS

LIST OF TABLES

LIST OF FIGURES

CHAPTER 1

INTRODUCTION

The national capital of India, Delhi, is bordered by the states of Haryana and Uttar Pradesh. With a maximum length of 51.90 kilometres and a width of 48.48 kilometres, the net area is 1,483 square kilometres. It is situated on the right bank of the Yamuna River, on the outskirts of the Gangetic plains. On the west and south west of Delhi, the huge Indian Thar desert of Rajasthan lies, and to the east, the Yamuna River, along which today's Greater Delhi has expanded. The Aravalli mountain range's ridges run across Delhi, along the west side of the city, and generate undulations in several areas of the state. The Yamuna river meanders between the Wazirabad and Mehrauli ridges in the north and the Mehrauli ridge in the south.

1. DELHI'S PHYSICAL CHARACTERISTICS

1.1. DELHI'S GEOMORPHOLOGY

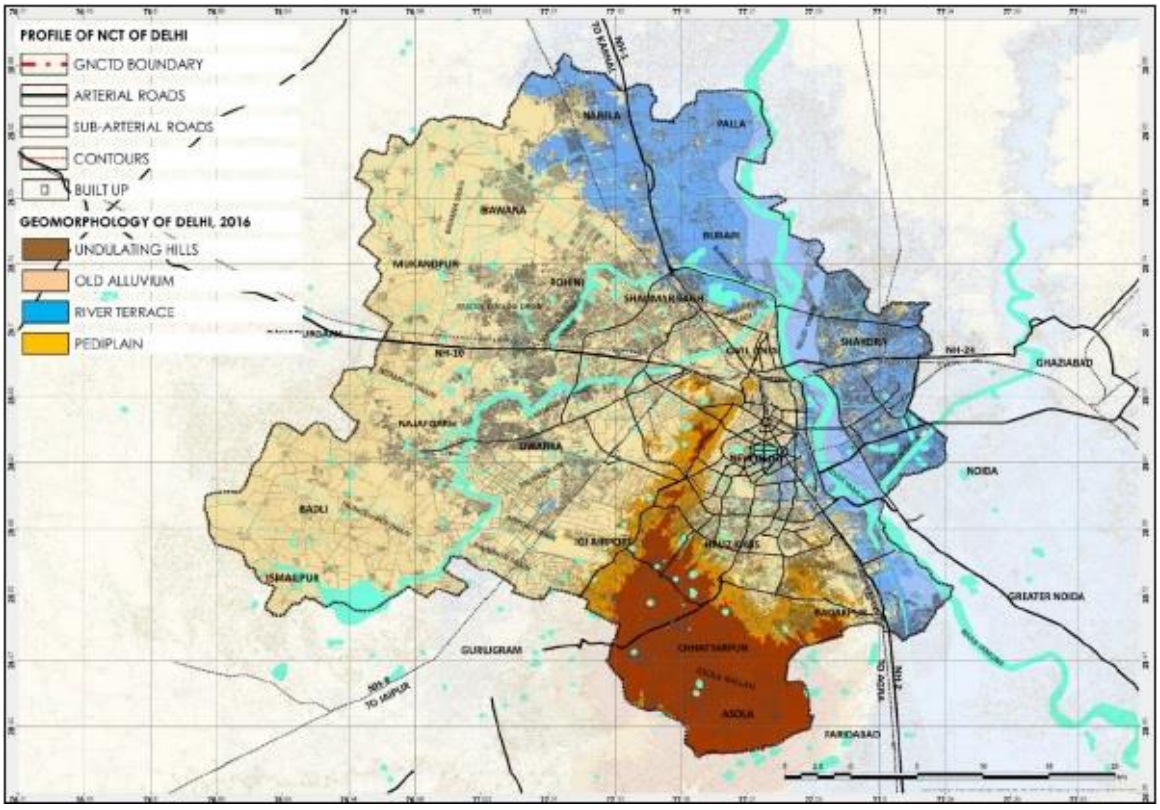

Figure 1: Geomorphology of Delhi (Adapted from: Report on Impact of Floods on Delhi (2017), School of Planning and Architecture, New Delhi)

Along the North and East region, Delhi is bounded by Indo-Gangetic alluvial plains and along its Western region, it is bounded by the old alluvium and by the Aravalli hill range in the South. The terrain of Delhi is flat except for the low North East and South West ridge which is considered an extension of the Aravalli hills of Rajasthan. The ridge is considered to enter Delhi from the South West. The eastern part of the ridge extends up to Okhla in the South and disappears below Yamuna alluvium in the North East on the right bank of the river.

1.2. DELHI'S HYDROLOGY

Potable water is at a depth of 60 m below the G.L. for approximately 90 percent of the city. For 10 % of city's limits comprising of the Ridge does not have suitable water recharge or aquifer and the remainder has saline and brackish water. The area covered by younger alluvium has the groundwater potential to yield 800 liters per meter (lpm) to 3200 lpm. The yield of old alluvium is 400 lpm to 500 lpm. Yield for the fringe area is low at 150 lpm to 300 lpm and while it is 100 lpm to 150 lpm for Delhi quartzite or the area under Delhi ridge.

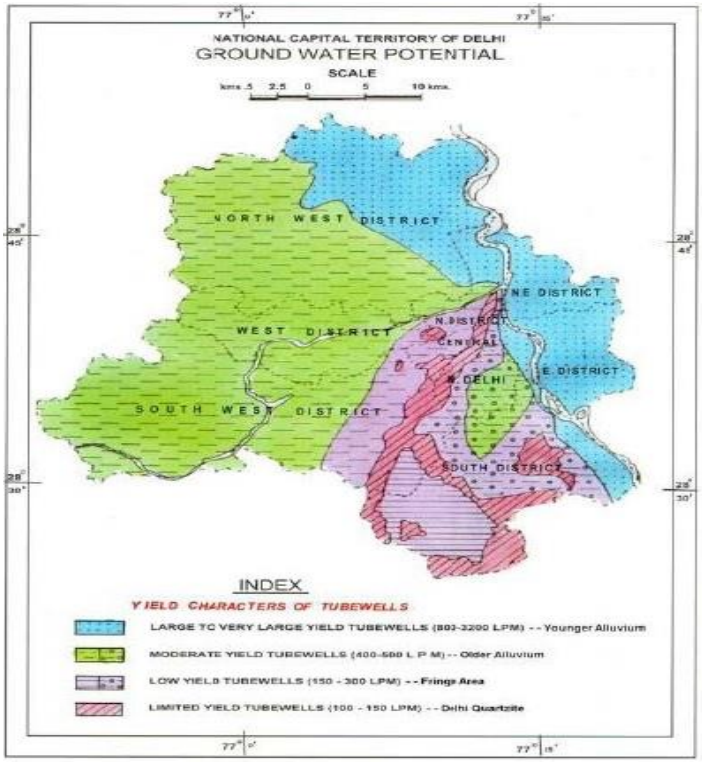

Figure 2: Groundwater Potential of Delhi (Adapted from: Report on Impact of Floods on Delhi (2017), School of Planning and Architecture, New Delhi)

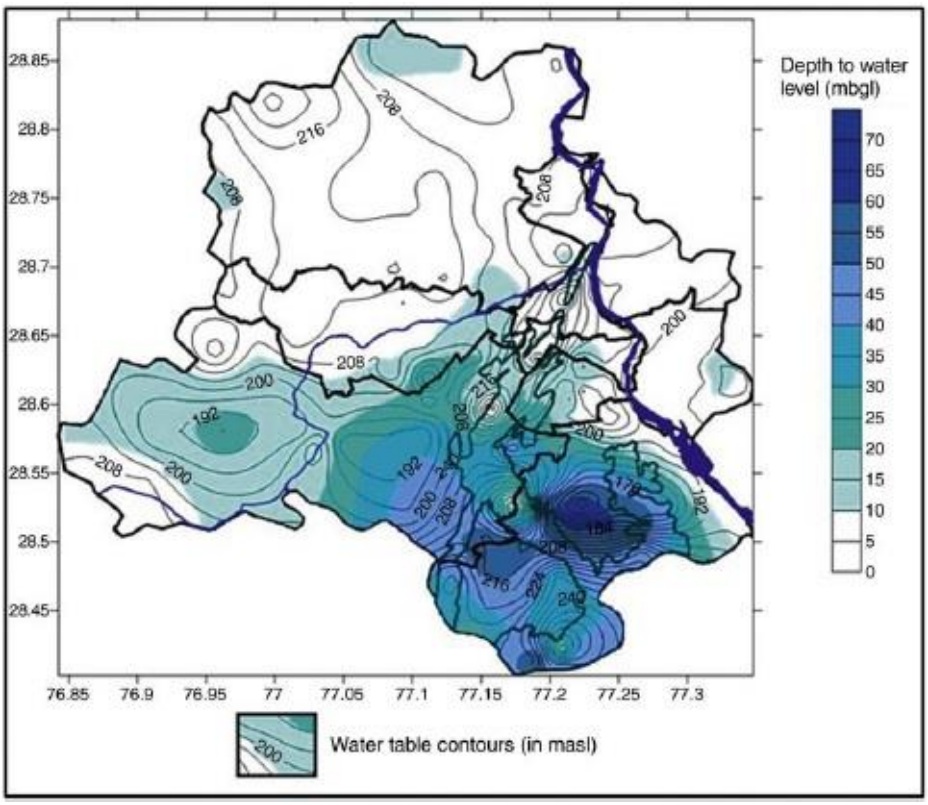

Figure 3: Hydrology of Delhi (Adapted from: Report on Impact of Floods on Delhi (2017), School of Planning and Architecture, New Delhi)

1.3. DELHI'S LAND USE PATTERN

Table 1: Land Use Pattern of Delhi (Adapted from: Report on Impact of Floods on Delhi (2017), School of Planning and Architecture, New Delhi)

Land Use	Area (in sqkm)	%
Residential Use	549	37.0
Commercial Use	53	3.6
Industrial Use	46	3.1
Public Semi-Public Use	103	7.0
Recreation	182	12.3
Transportation	148	10.0
Utility	36	2.4
Government Use	55	3.7
TOTAL =	1,483	100

The city of Delhi has been divided into nine use zones according to the master plan. Residential usage accounts for 63 percent of the city's land use, with recreation accounting for 21 percent and transportation accounting for 17 percent of the city's total developed area. Due to the phasing out of industries from Delhi following a Supreme Court judgement in the 1990s, commercial consumption has remained at 6.1 percent, while industrial use has decreased to 5.3 percent.

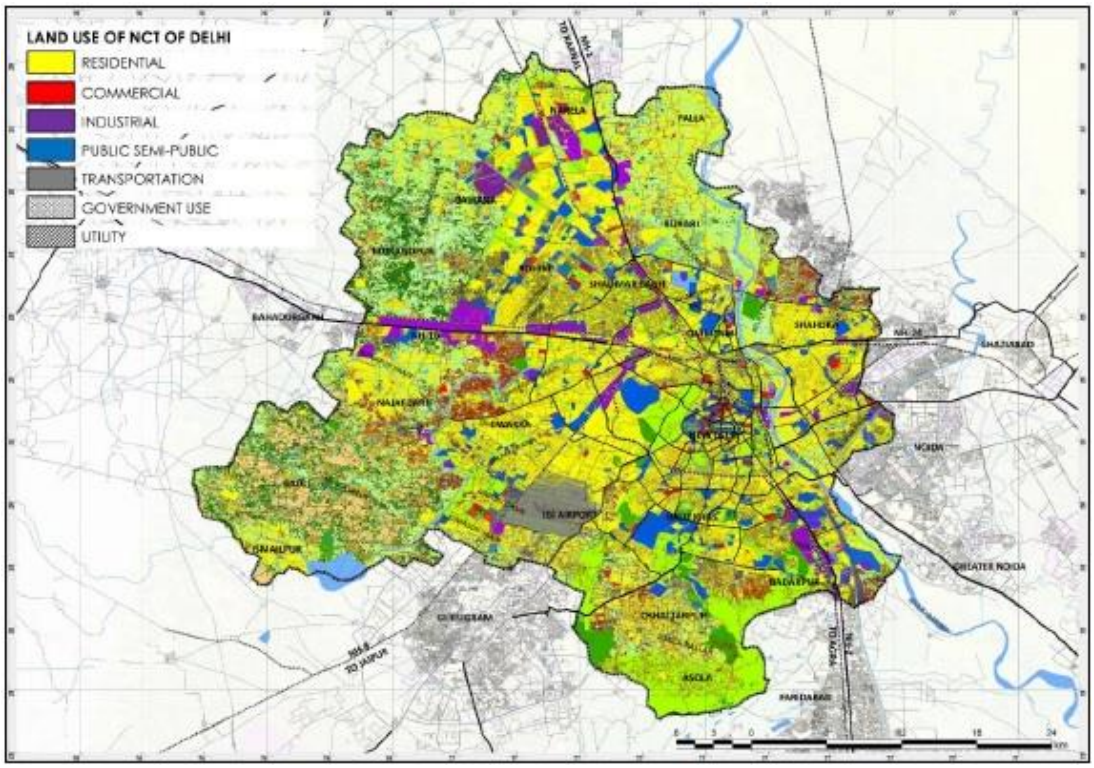

Figure 4: Land use Pattern of Delhi (Adapted from: Report on Impact of Floods on Delhi (2017), School of Planning and Architecture, New Delhi)

A comparison on Delhi's growth between 1989 and 2011 was done using Landsat Images. The basis of the study was to detect the changing land cover around Delhi using temporal data of Landsat TM5 (Thematic Mapper 5). Through the study it was concluded that there has been a rapid change in land cover/land use. Also an extensive variation in the built-up area in watersheds, loss of forest cover and a change of agricultural land.

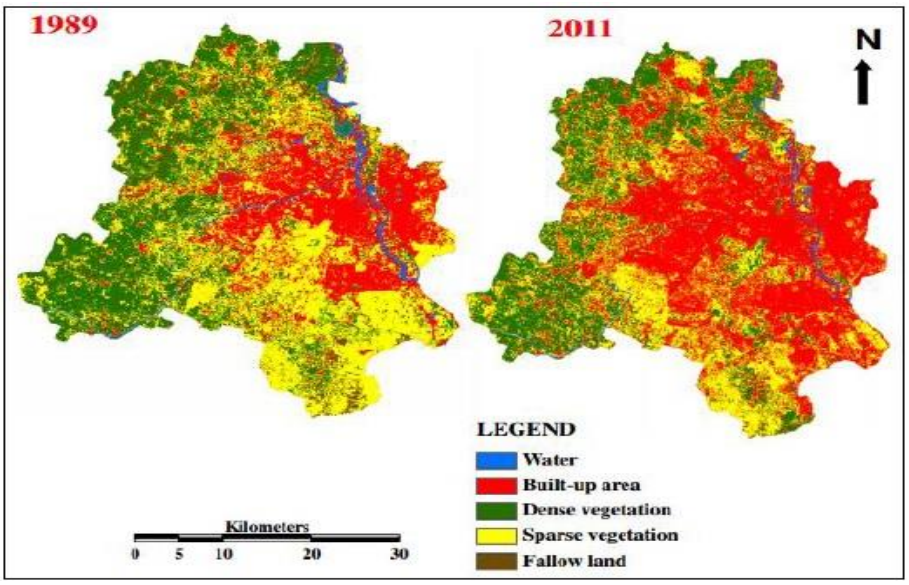

Figure 5: Land use – Land cover map (1989 and 2011) (Adapted from: Report on Impact of Floods on Delhi (2017), School of Planning and Architecture, New Delhi)

Public, semi-public use includes 12 percent of city's developed area while area under utilities and government use equals to 4.2 percent and 6.4 percent respectively.

1.4. DELHI'S TRANSPORTATION NETWORK

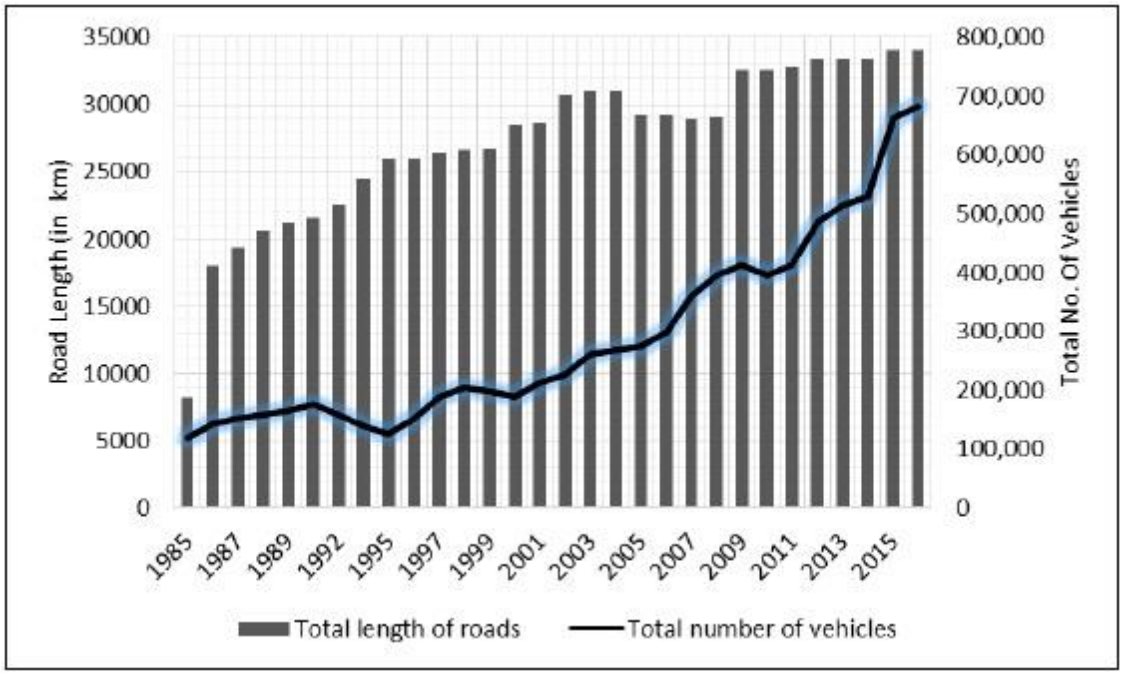

Figure 6: Growth of road network and vehicles in Delhi (1985-2016) (Adapted from: Report on Impact of Floods on Delhi (2017), School of Planning and Architecture, New Delhi)

Delhi contains of a vast hierarchical transportation network of national highways, arterial roads, sub-arterials, collectors and local roads at neighbourhood level. The total length of this network has increased to 34,012 km in 2016 from 8,231 km in 1985.

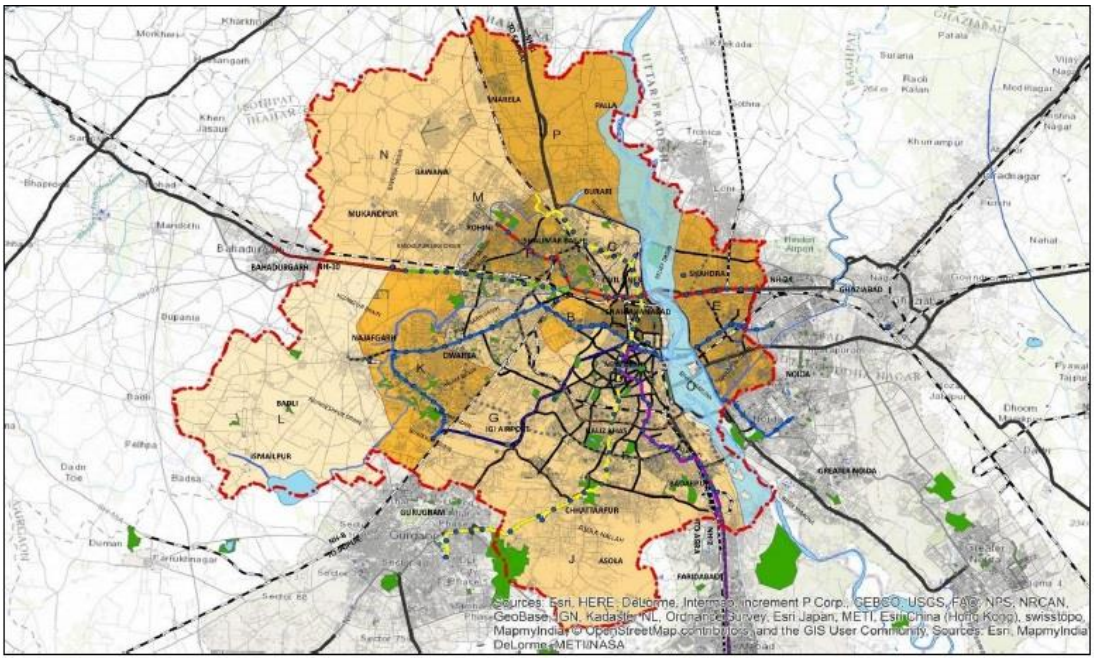

Figure 7: Transportation system of Delhi (Adapted from: Report on Impact of Floods on Delhi (2017), School of Planning and Architecture, New Delhi)

Delhi is connected by national highways which connect the city with cities and regions beyond its administrative boundary. Apart from national highways, the intra-city connections are supported by network of arterial roads which are fed by collector roads at community and local roads at neighbourhood level. The city's mobility even depends on the metro and Delhi Transportation Corporation plied bus network that cover a major part of Delhi. Apart from this the city is also dominated by private vehicles, cab services, e-rickshaws, auto rickshaws and cycle rickshaws.

1.5. DELHI'S DRAINAGE PATTERN

The city comprises of 24,840 hectares of flood plains of which 68 percent forms a part of Yamuna river floodplains. Based on the watershed of drains, the city has three drainage basins which includes North basin with a basin area of 26,694 hectares, west basin with an area of 5,633 hectares and a south

and east basin spread over an area of 45,973 hectares. According to the 2014 supreme court order, 300 m of flood plains in Delhi are delineated on either side of Yamuna river, 100 m on either side of the drains feeding Yamuna and 50 m for tertiary drains and water bodies like lakes and ponds. However, the flood plains have reduced in width from an average 800 m in 1986 to an average of 300 m in 2016 as a result of construction and developments that came up to the flood plains and resultant loss of the eco-fragile ecosystem.

Table 2: Engineered Storm Runoff System of Delhi

S. No	ZONE	No. OF DRAINS	TOTAL LENGTH OF DRAINS (km)
1.	Central	41	47
2.	South	127	102
3.	Sadar Paharganj	10	4.5
4.	Karol Bagh	47	23
5.	City Zone	10	8.6
6.	Civil Lines	77	339
7.	Shahadra South	174	134
8.	Shahadra North	197	135
9.	Narela	84	83
10.	Rohini	142	180
11.	West	185	410
12.	Najafgarh	185	410
	TOTAL	**1296**	**1694.1**

The demarcation of the city is done into six drainage zones namely, North, West, Central North West and South East, Central South and South East, East and South zone, by the Irrigation and Flood Control Department, Government of NCT of Delhi. Also to manage the storm runoff emanating from the entire urban expense, Delhi is divided into 12 municipal zones, which is carried by a total 350 km of natural drainage lines and a cumulative length of 1700 km of engineered storm water drains.

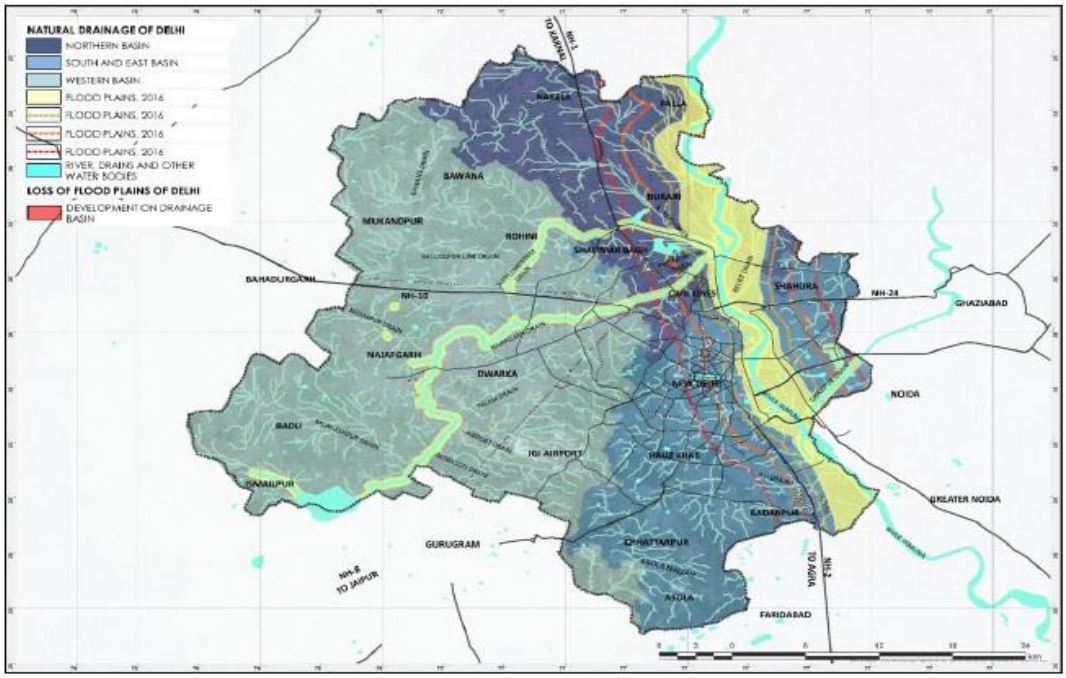

Figure 8: Drainage Pattern of Delhi and its Flood Plains (Adapted from: Report on Impact of Floods on Delhi (2017), School of Planning and Architecture, New Delhi)

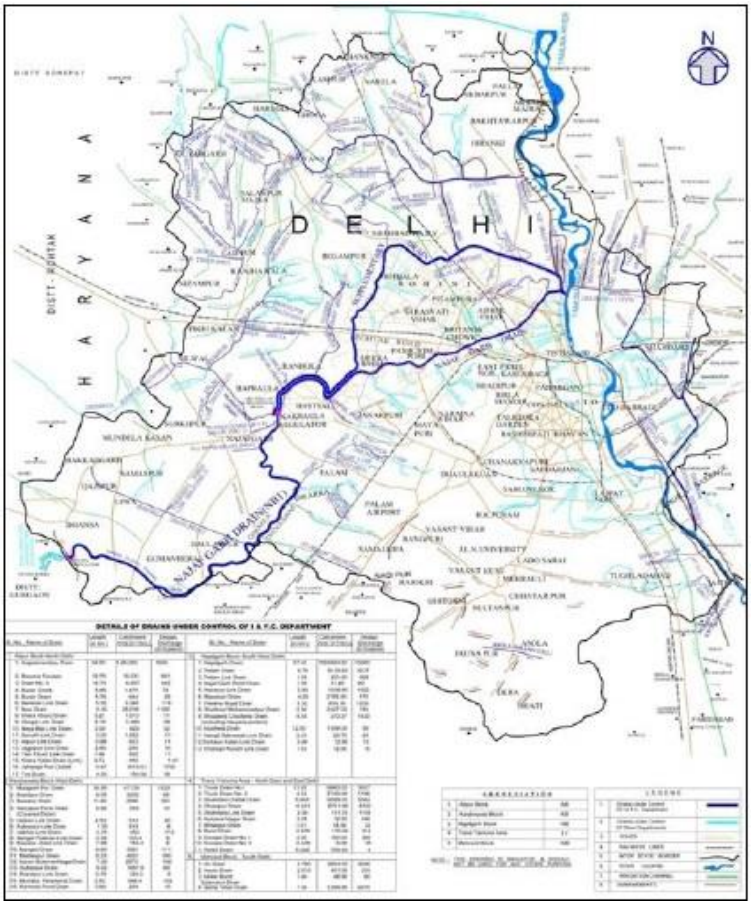

Figure 9: Drainage Pattern of Delhi as per Drainage Master Plan of 1976 (Adapted from: Report on Impact of Floods on Delhi (2017), School of Planning and Architecture, New Delhi)

2. FLOOD PATTERN OF DELHI

2.1. TREND OF ANNUAL PRECIPITATION

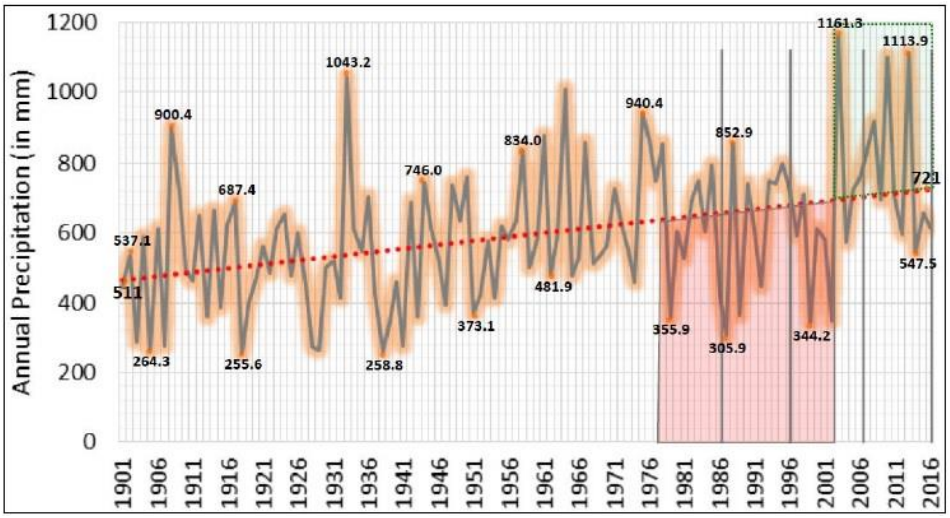

Figure 10: Change in Annual Precipitation of Delhi, 1901-2016 (Adapted from: Report on Impact of Floods on Delhi (2017), School of Planning and Architecture, New Delhi)

From 1901 to 2016, an assessment of annual rainfall and annual number of rainy was conducted. Its trend 1901 indicates that the average rainfall increased by 210 mm while drought periods have increased than rainfall periods. Assessing the trend of number of rain days for Delhi, the number of rainy days has increased by 9 rainy days and the average precipitation per rainy day has increased by 2.5 percent.

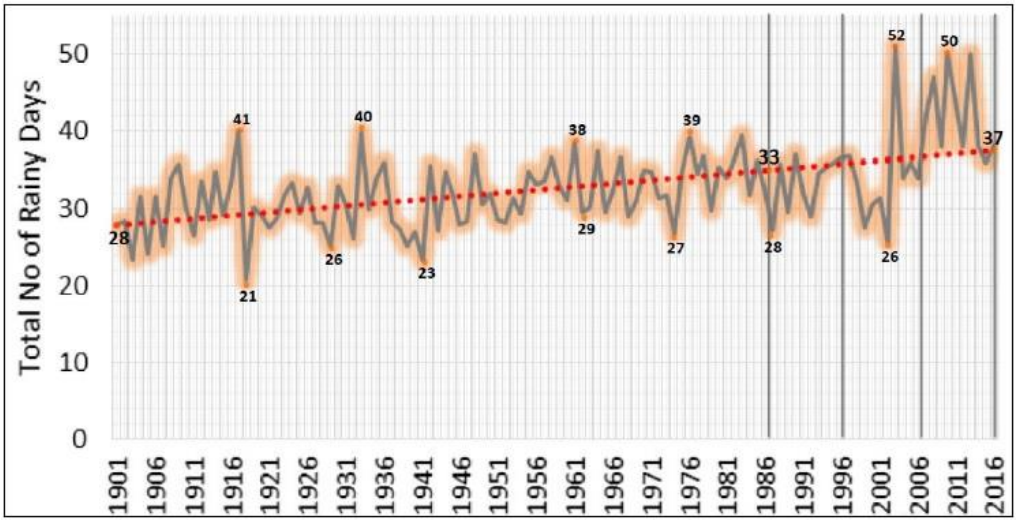

Figure 11: Change in Annual Number of Rainy Days for Delhi, 1901-2016 (Adapted from: Report on Impact of Floods on Delhi (2017), School of Planning and Architecture, New Delhi)

The annual precipitation and number of rainy days are increasing whereas the actual duration of precipitation has reduced leading to a sharp rise in the rainfall intensity from 13.2 mm/hr in 1986 to 22.9 mm/hr in 2016, leading to an inundation of over 50 percent of city in 2016 in three hours.

2.2. DELHI'S SEASONAL PRECIPITATION VARIABILITY

The seasonal precipitation variability is assessed in terms of seasonal share of annual precipitation and rainy days for the timeframe of 115 years (1901-2016). Analysis of seasonal share of annual precipitation indicates a trends of wetter summers and drier post monsoons.

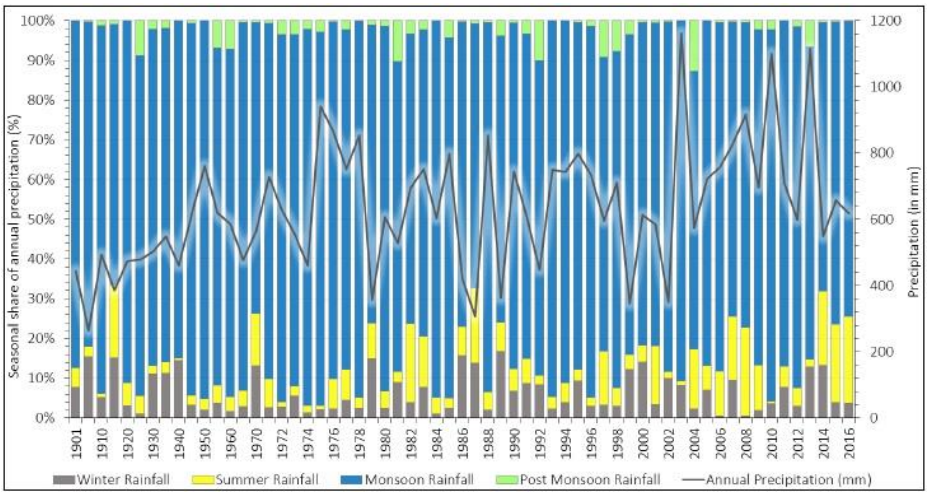

Figure 12: Seasonal Share of Annual Precipitation for Delhi, 1901-2016 (Adapted from: Report on Impact of Floods on Delhi (2017), School of Planning and Architecture, New Delhi)

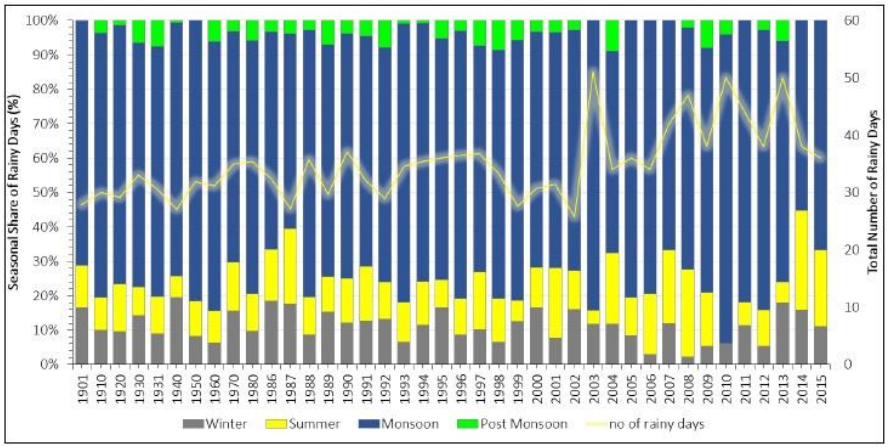

Figure 13: Delhi's Seasonal Share of Annual Number of Rainy Days, 1901-2016 (Adapted from: Report on Impact of Floods on Delhi (2017), School of Planning and Architecture, New Delhi)

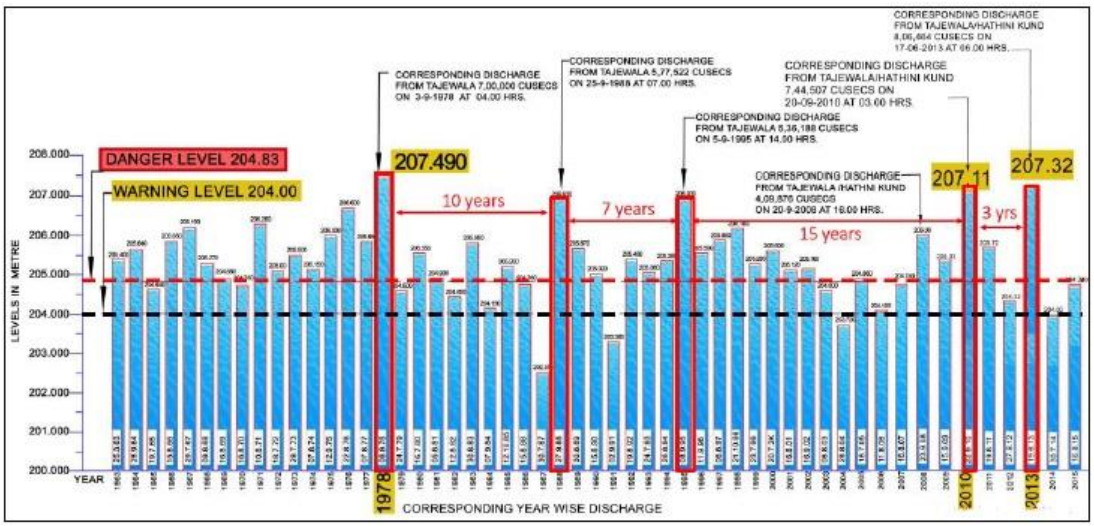

Figure 14: Delhi's Seasonal Share of Annual Number of Rainy Days, 1901-2016 (Adapted from: Report on Impact of Floods on Delhi (2017), School of Planning and Architecture, New Delhi)

This analysis depicts that summer are getting wetter whereas winters and post monsoon rainfall is decreasing. Rainy days are also decreasing, while real precipitation duration is increasing, resulting in an increase in rainfall intensity from 13.2 mm/hr in 1986 to 22.6 mm/hr in 2016. In 2016, three hours of this intensity of rainfall inundated more than half of the city, disrupting movement and livelihoods.

2.3. DELHI'S PAST TRENDS OF FLOODS

Delhi has become vulnerable to climate related hazards such as floods caused by unpredictable rainfall patterns. The city has experienced floods in the past due to floods in rivers Yamuna and Sahibi (through Najafgarh drain). The discharge from Tajewala Headwork (240 km upstream) influences the flow in river Yamuna. In case of heavy rainfall event, excess water from Tajewala is released which takes about 48 hours for Yamuna level in Delhi to rise. A backflow in city's drains are experienced due to the rise of the water level. Since 1900, the city has experienced nine major floods in the years, 1924, 1947, 1976, 1978, 1988, 1995, 1998, 2010 and 2013 when the river's head crossed the danger level of 204.83 m.

Delhi's North East, Central, South East and East districts are most vulnerable to flooding. During the monsoon season, low lying areas (specially in East Delhi) are most prone to floods. During the 2010 Delhi floods, a heavy damage to life and property was recorded in which hundreds of settlements got submerged under water and government had to set up 169 relief camps.

2.4. DISCHARGE IN RIVER YAMUNA

Meteorological estimates suggest that precipitation, number of rainy days coupled with reduction in rainfall duration per day, rainfall intensity and surface runoff has increased significantly. There is a cumulative impact on discharge of Yamuna river since it receives water from Hathnikund barrage in the state of Haryana as well as drains and surface runoff from the city of Delhi. As the surface runoff increases, the actual amount of water that reaches river gets reduced due to increasing impermeable surface or loss in continuity of water. Consequently, the actual quantum of discharge gets reduced gradually whereas the flooding and precipitation increases.

2.5. IMPACT OF FLOODS

The uneven distribution of rainfall along with unplanned urbanisation, illegal encroachments filling up the natural drainage channels and urban lakes over high value land for buildings cause an increase in flood incidences in the city. There is rampant illegal filing of urban water bodies in Delhi. The water bodies of Delhi have reduced from 800 to 600. Numerous illegal colonies have emerged in the city resulting in narrowing of natural drainage posing a serious health of the city and invitation to urban flooding.

2.6. IMPACT OF FLOOD ON THE ROAD NETWORK AND TRAVEL PATTERN

Based on various newspaper reports and recent studies, observations for water logging areas revealed that after 5mm of rainfall, increase in every 1mm rainfall there will be 2 min of additional time increase in the network and same is adopted for the study to understand the travel pattern during the flood time.

Table 3: Impact of Rainfall on Road Network and Travel Time

IDENTIFIED ROUTES	NORMAL DAY (TT in Mins)	RAINY DAY (TT in Mins)	RAINFALL (mm)
Lajpat Nagar – Ashram	30	90	26
Faridabad from Connaught Place	42	90	22
ITO from South Extension	40	90	26
Average	37	90	25
Impact of Rainfall on Travel Time (TT)		**2.41**	
1 mm rainfall will increase in TT by		**2.11**	1 MM
5 MM	48		
10 MM	58		
15 MM	69	1.85	

3. FLOOD FORECASTING

Floods wreak havoc on crops and precious assets, as well as wreak havoc on people's lives. In India, 40 million hectares of area has been identified as vulnerable. Since a large river system lies in India, seasonal floods are often experienced in India. Floods occur every year in one part or the other of the country. In the months of July, August and September the North and Central Indian rivers are prone to regular floods. In late May, Brahmaputra river basin experiences floods. While Southern Indian rivers continue to flood till November. Floods affect around 33 million people between 1953 – 2000.

The occurrence of floods is due to natural and manmade reasons. Heavy precipitation, insufficient riverbank capacity to contain high flows, excessive silting of riverbeds, landslides obstructing flow and changing river course, tidal and backwater effects, poor natural drainage, cyclone and heavy rainstorms/cloud bursts, snowmelt and glacial lake outbursts, and dam break flow are all major causes of floods.

Various flood control techniques, commonly known as "Flood Management," can be designed using structural or non-structural means to limit loss due to floods.

Construction of multipurpose reservoirs and retarding structures to store flood waters, channel improvements to increase river flood carrying capacity, embankment and levees to keep water away from flood prone areas, detention basins to delay and absorb some flood water, flood ways to divert flood flows from one channel to another, and overall drainage system improvement are all structural measures. Flood protection covered nearly 13 million hectares of land until 1985. In India, no systematic investigation of the efficacy of these structures on river flow regimes during floods has been conducted. As a result, most of the places will be unprotected for a long time.

Due to budgetary limits, cost-benefit factors, or topographic limitations of the region, permanent flood protection by structural methods is not practicable nor viable. Non-structural flood management strategies include real-time flood predictions and flood plain zoning. The method of estimating the future stage of flows and their time sequence at designated susceptible places along a river's path during floods is known as "Real Time Flood Forecasting". These are prepared to issue floods in real time so as to prepare evacuation plan during floods. If these flood warning are received well on time, people can be relocated to safer place as well. The accuracy of this flood forecasting technique is determined by how well the future stage or flow of an oncoming flood, as well as its temporal sequence at various locations along the river, can be anticipated. Because the lead time for flash flood predicting is so short, it's impossible to have an evacuation strategy in place.

The techniques for real time flash flood forecasting are as follows:

i. Deterministic modelling
ii. Stochastic modelling
iii. Statistical modelling
iv. Computational techniques.

Index catchment models and conceptual catchment models are examples of deterministic models. These are more likely to replicate the reaction of a basin to hydrological events than to completely utilise data acquired during an event. These models were created for design studies and are not used to provide real-time hydrological data. These models are difficult to update and may be difficult to reinitialize during telemetry or a computer failure.

The stochastic hydrological models with structures more suitable to real-time forecasting overcame the inadequacies of the deterministic hydrological models. These were developed in the 1970s and have been used successfully for real-time forecasting. These build links between the flood characteristics of forecasting stations and upstream gauging stations, taking into account numerous flood-related elements.

Flood forecasting approaches in India are based on the availability of hydrological and hydro meteorological data, basin features, computing resources available at forecasting stations, needed warning time, and forecasting objective. The following approaches were used:

i. simple relation correlating the stage-discharge data
ii. co-axial correlation diagrams developed utilizing the stage
iii. discharge and rainfall data
iv. event based hydrological systems models for small to moderate sized catchments
v. hydrological models

3.1. NEED FOR FLOOD FORECASTING

The following are the reasons for flood forecasting:

- People's evacuation to safer place
- Execute flood protection projects, such as embankments, to prevent breaches, failures, and other problems.
- In case of higher return period floods, ensure the regulation of floods through the barrages and reservoirs.
- Operation of multifunctional reservoirs such that encroachment into the power and water storage systems may be avoided in order to regulate incoming floods
- To prevent the bank flow and flooding of the areas drained by them by properly operating the city drains.

3.2. DEVELOPMENT OF FLOOD FORECASTING IN INDIA

The government of India created a Central Flood Forecasting Directorate in 1969. It was headed by a superintending engineer. Under Member (Floods), six flood forecasting divisions were set up on interstate river basins including the basins of Ganga, Brahmaputra, Narmada, Tapti, Teesta and the coastal rivers of Orissa in1970.

There are flood warning from the upstream stations to the downstream stations. The warnings may include:

i. If the river is rising above the danger level or not

ii. If the river level is rising or falling

iii. If the river's stage is low, medium or high

These warnings are issued by telegram, telephone or wireless systems and provide an indication of the nature of the flood. It is being used in the states of West Bengal, Andhra Pradesh and Bihar.

4. ENSEMBLE FRAMEWORK FOR FLASH FLOOD FORECASTING

The University of Oklahoma and the National Aeronautics and Space Administration (NASA) created Coupled Routing and Excess Storage (CREST) hydrological model and the Ensemble Framework for Flash Flood Forecasting (EF5) software to overcome the issue of flooding. For that data such as precipitation, evapotranspiration and stream flows are required. EF5 incorporated CREST water balance model, SAC-SMA water balance model and then have the runoff output from either of those forcing a river routing scheme. Because of their overall computing efficiency, kinematic and linear reservoir routing were the first river routing systems devised. With the continued use of this software, need for snow parameterization and calibration was desirable so Snow -17 parametric temperature index snow model and DREAM automatic calibration were added to it.

Basic files such as Digital Elevation Map (DEM), Flow Direction Map (FDR) and Flow Accumulation Map (FAC) are required to pick an area to model. Since, EF5 is resolution independent, it works with any DEM resolution between 0.5 m to 12 km. Gauge is the downstream point to model and it may or may not correspond with the observation measurement location. One may also model on a group of gauges. The

model's parameters are defined each gauge and then applied as a simple multiplier to the scattered values wherever upstream of the gauge till the next gauge arrives.

EF5 is developed in C++ and has a total of 20,388 lines of code, and it supports Linux, Mac OS X, and Windows. Linux and Mac OS X are supported through a binary that may be executed from a shell command prompt, although Windows has a complete graphical user interface (GUI). When compared to Linux and Mac OS X versions, the Windows GUI delivers a fairly similar visual feedback and is easier to deal with.

EF5 now supports a wide range of file types and projections. The recommended format is Geotiff, which has the particular benefit of containing native compression capabilities, resulting in a significant reduction in file size. For all gridded fields, ESRI Arc ASCII grids are also provided as input choices. For precipitation, MRMS binary and TRMM TMPA 3B42 real time binary are supported. GIS tools such as GDAL can easily convert GPM Geotiffs to EF5 compliant formats.

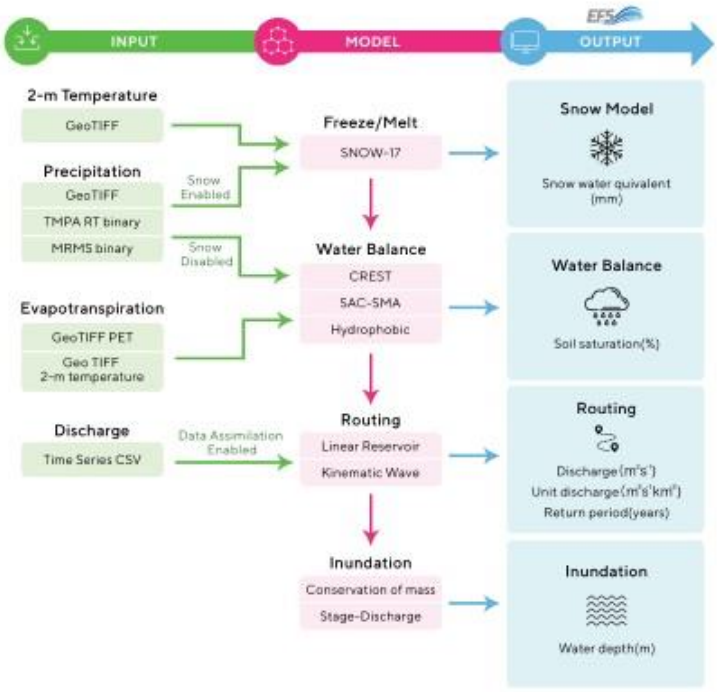

Figure 15: EF5 flowchart showing the many modules and choices available. The arrow depicts the pathways that input data can take to transit between modules.

Through virtual base classes for snow melt, water balance, and routing physics, EF5 offers a variety of model physics. Precipitation and potential evapotranspiration are two input driving factors for the water balance component, with fast flow

component (surface flow), slow flow component (subsurface flow), and soil saturation value as output variables.

The basic class has methods for starting the model, initialising model state variables that may have been saved to file, saving model state variables to file, and lastly conducting the water balance physics. The route and snow components have similar implementation methods as the water balance component, including start up, state loading, and saving the main method for physics execution. The routing virtual class accepts both fast and slow flow inputs and outputs a single discharge variable. Precipitation and temperature are inputs to the snow modules, with melted runoff and snow water equivalent as output variables.

Because of the model physics implementation, EF5 can simply extend in the future to include more options for treating basic hydrologic processes. This feature is crucial because it allows new physics to be introduced to practical flood forecasting systems in the future without requiring a major rebuild of the supporting infrastructure.

4.1. WATER BALANCE MODELS

The three water balance models included in EF5 are theoretically based and rely on parameters that are guided by land surface and subsurface variables determined from current data sources. CREST, SAC-SMA, and hydrophobic are the three possibilities (HP).

4.1.1. Hydrophobic (HP)

It is the simplest model since no parameters are to be specified for the land surface. Because the surface is assumed to be entirely impervious in this model, all rain quickly runs off and downslope. When running in an ensemble with other water balance models, this water balance model is included for the ability to diagnose processes and faults. Underestimation of this model indicates that the precipitation is likely biased. It produces an upper bound on the expected discharge values. When the model solutions match with the observed streamflow then

either the entire drainage area is acting as an impervious surface or the inputs into the model are underestimating the magnitude of the rainfall.

This model can also be used to approximate the land surface response after wildfires when the soils become hydrophobic. Most realistic simulations from this model are mostly comprised of the burn areas. Running EF5 in an ensemble with all three models allow for the impacts of the wildfires to be accounted for without having to modify distributed model parameter grids. This allows for quicker operational response to changing land surface conditions in the event of wildfires that is proceeded immediately by heavy rainfall events.

4.1.2. Coupled Routing and Excess Storage (CREST)

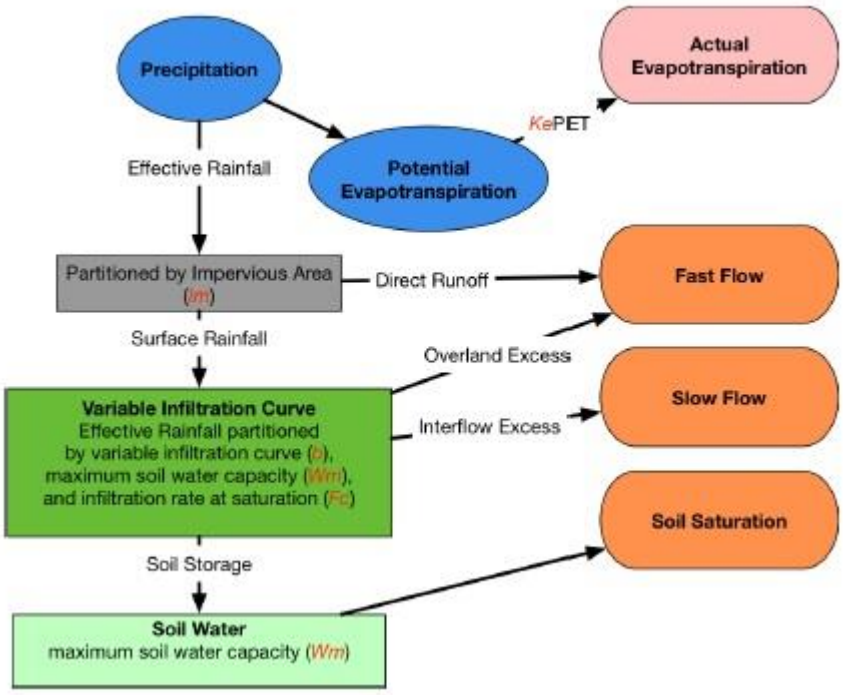

Figure 16: The succession of processes reflected in the EF5/CREST water balance component is depicted in this diagram.

It is a derivation of the Xinanjiang model, which contains a variable infiltration curve for partitioning rainfall into direct runoff and infiltration and was created for use in China. The original version was published in (Wang et al., 2011), and the version used here is an adaption of that.

There is only one soil layer in the EF5/CREST implementation, further simplifying the model and lowering the input data requirements. Partitioning for impervious area is also included in EF5/CREST.

As EF5/CREST is different from earlier versions of CREST, a full description of the model is provided here. The first stage, as illustrated in equation 1, is to convert potential evapotranspiration to effective evapotranspiration by employing a scalar parameter called Ke. When employing distributed potential evapotranspiration without model calibration, the Ke parameter is commonly set to 1.

$$EET_t = K_e + PET_t \quad (1)$$

EET_t is the effective evapotranspiration, while PET_t is the input forcing data into EF5. The Penman-Monteith equation, which calculates potential evapotranspiration as a function of air temperature, is frequently used to calculate PET_t in EF5/CREST. The monthly mean or even hourly PET for use with EF5 may then be computed using climatology of air temperature.

$$EP_t = \begin{cases} 0, & \text{for } EET_t \geq P_t \\ P_t - EET_t, & \text{for } EET_t < P_t \end{cases} \quad (2)$$

P_t is the amount of rainfall that is forced into EF5. The direct runoff is estimated from the effective rainfall (EP_t), with the remainder falling to the soil and subsequently the infiltration process. The rainfall is then divided into three parts: that which reaches the soil (SP_t), that which contributes to real ET, and that which contributes to direct runoff (DP_t)

$$DP_t = EP_t + I_m \quad (3)$$

$$SP_t = EP_t * (1 - I_m) \quad (4)$$

The percent impervious area is represented by the scalar parameter I_m. The I_m parameter is calculated using satellite-based land cover maps, which identify cities where land has been converted to impermeable surfaces as a result of human activity. The satellite LULC maps usually have a very fine resolution, which may be averaged with the model's coarser resolution to get the proportion of impervious area per grid cell. The infiltration is then modelled using the following formula:

$$I_t = \begin{cases} 0, & \text{for } P_t \leq EET_t \vee SM_t \geq W_m \\ W_m - SM_t, & \text{for } (i_t + SP_t) \geq I_m \\ W_m - SM_t - W_m * [1 - \frac{i_t + SP_t}{i_m}]^{1+b}, & \text{for } (i_t + SP_t) < I_m \end{cases} \quad (5)$$

W_m stands for maximum water capacity, SM_t for soil moisture status variable, and b for the variable infiltration curve exponent. Both W_m and b are changeable parameters in EF5/CREST, however they are frequently defined apriori. i_m stands for maximum infiltration capacity, which is defined as:

$$i_m = W_m * (1+b) \quad (6)$$

The current infiltration capability, it is defined as follows:

$$i_t = i_m * [1 - (1 - \frac{SM_t}{W_m})^{\frac{1}{1+b}}] \quad (7)$$

Based on the infiltration, the effective precipitation is subsequently partitioned into excess rainfall (ER_t).

$$ER_t = \begin{cases} 0, & \text{for } SP_t = 0 \vee SP_t \leq I_t \\ SP_t - I_t, & \text{for } SP_t > I_t \end{cases} \quad (8)$$

Overland (OER_t) and subsurface (SER_t) flow components are separated from the surplus rainfall by:

$$SER_t = \begin{cases} 0, & \text{for } EP_t = 0 \\ temX_t, & \text{for } ER_t > temX_t \\ ER_t, & \text{for } ER_t \leq temX_t \end{cases} \quad (9)$$

With $temX_t$ is defined as:

$$temX_t = \begin{cases} \frac{SM_t + W_t}{2W_m} * F_c, & \text{for } EP_t > 0 \\ (EET_t - P_t) * \frac{SM_t}{W_m}, & \text{for } EP_t = 0 \end{cases} \quad (10)$$

Using F_c to represent the hydraulic conductivity and with W_t as:

$$W_t = \begin{cases} 0, & \text{for } EP_t = 0 \\ W_m, & \text{for } SM_t + I_t \geq W_m \\ SM_t + I_t, & \text{for } SM_t + I_t < W_m \end{cases} \quad (11)$$

The difference between the quantity that infiltrates and the extra rain, plus the direct runoff, is used to compute the overland flow component.

$$OER_t = \begin{cases} 0, & \text{for } EP_t = 0 \\ ER_t - SER_t + DP_t, & \text{for } EP_t > 0 \end{cases} \quad (12)$$

The new soil moisture value is then computed using:

$$SM_{t+1} = \begin{cases} SM_t - temX_t, & \text{for } EP_t = 0 \\ W_t, & \text{for } EP_t > 0 \end{cases} \quad (13)$$

Finally, the actual evapotranspiration, AET_t is given as:

$$AET_t = \begin{cases} temX_t & \text{for } EP_t = 0 \\ EET_t, & \text{for } EP_t > 0 \end{cases} \quad (14)$$

There are six parameters that may be changed in this model. W_m is the cell's maximum water capacity, which is proportional to the porosity of the soil in the first 50 to 100 cm. When the grid cell is saturated, F_c is the maximum quantity of water that can infiltrate into the subsurface flow. K_e is a linear adjustment to prospective evapotranspiration that regulates the efficiency with which potential evapotranspiration is converted to actual evapotranspiration. The *b* parameter has to do with the texture of the soil. The percentage of rain that is converted directly to overland drainage is known as I_m. This parameter is related to impervious area of the grid cell. I_{wu} is the percent W_m that is water initially in the grid cell. This is really a model state, but to allow for more thorough model calibration is classed as a parameter value.

4.1.3. Sacramento Soil Moisture Accounting (SAC-SMA)

It is the most complex model used in EF5. It is based on Korean et al. (2004) and Yilmaz et al. (2008). In comparison to EF5/CREST, SAC-SMA has many zones with substantially more intricate interactions. This model generates runoff using a saturation excess mechanism rather than the infiltration excess method utilised in EF5/CREST. In addition, this model divides rainfall between impervious and permeable surfaces, with impervious areas directly contributing to runoff in each grid cell.

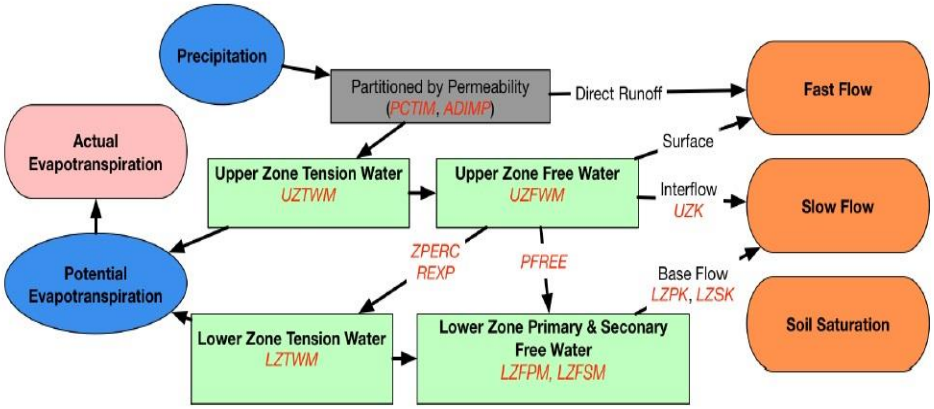

Figure 17: The EF5/SAC-SMA water balance component has a schematic depicting the flow of processes, inputs, and outputs.

An upper and bottom layer (zone) absorb and transport water in fundamentally distinct ways in this model. When precipitation occurs, the higher zone fills first and serves as a short-term storage capacity. The lower zone, which acts as the long-term storage capacity for the grid cell, serves to provide the base flow. Each zone is further subdivided into tension water which acts as surface tension and can only be removed from grid cell by evapotranspiration and free water which moves through the cell vertically to the lower zone from the upper zone or discharged as streamflow out of the grid cell.

4.2. ROUTING OPTIONS

4.2.1. Linear Reservoir

The routing options available are lumped routing model conceptualized as a series of linear reservoirs and a kinematic wave approximation of the Saint-Venant equations for one-dimensional open channel flow. The linear reservoir option is adopted from the original CREST model.

The EF5 linear reservoir option features two separate reservoirs where their depths are computed as:

$$OR_{t+1} = OR_t + OER_t + \sum_{i=1}^{N} OER_t^i \quad (15)$$

$$SR_{t+1} = SR_t + SER_t + \sum_{i=1}^{N} SER_t^i \quad (16)$$

The overland and subterranean reservoirs are represented by OR_t and SR_t, respectively. The extra rainfall components from EF5/CREST, OER_t and SER_t, indicate rapid and slow flow components, respectively. N is the number of nearby grid cells that flow into the current grid cell. The discharge from each reservoir is calculated as follows:

$$OQ_t = LeakO * OR_t \quad (17)$$

$$SQ_t = LeakI * SR_t \quad (18)$$

$$Q_t = OQ_t + SQ_t \quad (19)$$

LeakO and *LeakI* are parameters defining the rate of discharge. The total discharge Q_t is based on the simulation of the fast (OQ_t) and slow (SQ_t) discharge rates. At each step the fast and slow discharges are routes downstream following the FDM into the reservoir of the downstream grid cells.

4.2.2. Kinematic Wave

The implementation of this routing is based on an approximation of one dimensional unsteady open channel flow equations. In 1871, Barre de Saint-Venant developed full-one dimensional unsteady open channel flow equations which represented a physical description of the movement of water in a watershed. Its complete equations have a number of assumptions which must be met including flow in one dimensional, the flow varies gradually along the channel implying vertical accelerations can be neglected, the channel is approximately a straight line within a given grid cell, the channel does not experience scour or deposition and the flow fluid is incompressible implying a constant density. This model further simplifies the equations and requires that the bed slopes are steep. In case of steep slope, the kinematic wave approximation reasonably describes the unsteady flow phenomenon. The kinematic wave model is widely used in hydrology and has been implemented in systems such as the Hydrologic Engineering Centre's Hydrologic Modelling System, Storm Water Management Model created by Environmental Protection Agency, HL-RDHM previously mentioned here and described in Korean et al. (2004) and finally already coupled to the Xinanjiang model (Liu et al., 2009).

Deriving the kinematic wave approximation starts with Saint-Venant equations in the Eulerian frame of reference where we model fluids as it passes by control point, or in the case as it passes through a control volume. The time rate of change of fluid is modelled as a function of the external forces acting on it as Reynolds transport theorem (Chow et al.,

1988). Newton's second law is use to derive external forces, while neglecting lateral inflow, eddies and wind shear. The Saint-Venant continuity equation is given as:

$$\frac{\partial Q}{\partial x} + \frac{\partial A}{\partial t} = q \tag{20}$$

where *Q* is the discharge, *x* is the horizontal distance, *q* is the lateral inflow into the channel, *t* is time and the channel cross sectional area is A. The momentum equation is defined as:

$$\frac{1}{A}\frac{\partial Q}{\partial t} + \frac{1}{A}\frac{\partial}{\partial x}\left(\frac{Q^2}{A}\right) + g\frac{\partial y}{\partial x} - gS_o + gS_f = 0 \tag{21}$$

where gravity is *g*, S_o is the bottom channel slope, and S_f is the friction slope. Simplifications to equation 20 and 21 represent different schemes commonly used in distributed hydrologic models. When no simplifications are made then the routing is referred to as dynamic wave, when the acceleration terms are neglected the resulting wave model is called diffusive wave and when the acceleration terms are neglected and the gravity force and friction force are assumed equal the result us the kinematic wave routing. In kinematic wave assumption, the resulting equation for momentum is:

$$Q = \alpha A^{\beta} \tag{22}$$

where *α* and *β* are the kinematic wave parameters. This may be substituted back into the continuity equation and solved for *Q* which yields:

$$\frac{\partial Q}{\partial x} + \alpha\beta Q^{\beta-1}\frac{\partial Q}{\partial t} = q \tag{23}$$

Chow et al. (1988) provided implicit solutions for distributed routing which are implemented in EF5. The kinematic wave routing in EF5 is only applied to overland discharge, the subsurface discharge is routed

with linear reservoir routing. The above equations describe the kinematic wave routing for channel routing. for overland routing the process is same as above but for q instead of Q. the resulting equations is:

$$\frac{\partial q}{\partial x} + \alpha_0 \beta_0 q^{\beta_0 - 1} \frac{\partial q}{\partial t} = i - f \qquad (24)$$

where α_o is the overland conveyance parameter, β_o is fixed at 3/5. The i-f term is surface excess rainfall passed in from water balance model.

CHAPTER 2

LITERATURE REVIEW

Cloke and Pappenberger (2009) found that, rather than single deterministic forecasts, operational and research flood forecasting systems around the world are increasingly using ensembles of Numerical Weather Predictions (NWPs) known as Ensemble Prediction Systems (EPS) to drive their flood forecasting systems.

Wenyan Wu et al. (2020) found that improving technical elements of flood forecasting, as well as bridging the gap between scientific research communities and flood forecasters and managers, is necessary to boost the acceptance of ensemble flood forecasting in flood or water management.

Tomar et al. (2021) came to the conclusion that GIS is well adapted for developing floodplain management plans using post-disaster verification of floodplain extents and depths. They also created a basic framework that planners could use to access flood disaster risk reduction and augment current flood control infrastructure to assist them cope with floods more effectively.

Tiwari et al. (2010) found that using a bootstrap-based artificial neural network, small length data with adequate representation can generate better results than large length datasets; nevertheless, further research is needed to determine the ideal dataset length that causes the least amount of error. The rising limb of the water level hydrographs was likewise shown to be biased towards the higher confidence band, whilst the recession limb was found to be biased towards the lower confidence band. Furthermore, ensemble prediction revealed that the models underestimate the rising limb of the flow hydrograph while overestimating the falling limb, especially at higher water levels. This can be regarded as a pattern of expected values shifting. Bias correction strategies might be used in studies to rectify this shift.

Nanditha et al. (2021) found that there is a need to construct an ensemble flood forecasting system, which is the most effective flood forecasting system in the world. In addition, the Central Water Commission should update flood forecasting rules and lead efforts to establish and improve an ensemble flood forecasting system that takes advantage of the existing ensemble precipitation forecasting system.

Konstantinos et al. (2019) concluded that GloFAS as an operational warning system system in Peru showed large quantitative differences between the observed and simulated discharge data. This may be explained by the fact that this system is not calibrated for that area. The method is most commonly used in data-poor locations where high-quality, daily observational discharges are unavailable. It may also be applied to each river cell separately, allowing for a large-scale assessment of the model's competence.

Balint et al. (2006) found that using meteorological ensembles to generate sets of hydrological projections improved the capacity to deliver flood warnings.

Shi et al. (2015) concluded that SOA (service oriented architecture) will be a viable method for ensemble flood forecasting based on the NWP (numerical weather prediction), giving prospective victims considerably more time to react when faced with probable floods. This technique might be effective in hilly river basins for avoiding or decreasing flood disaster losses.

Roulin (2007) found that the hydrological ensemble forecasts were shown to be more accurate than deterministic predictions.

Liu et al. (2017) developed an ensemble flood forecasting system based on parallel automated calibration and multimodel ensemble approaches using the VIC hydrological model The findings underlined the necessity of a calibration technique for distributed hydrological models and ensemble methods in flood forecasting, and they might be effective in practise.

Bartholmes et al. (2009) concluded that the application of EPS in hydrological forecasting proven to be a significant benefit to a flood early warning system, with EPS-based predictions often outperforming deterministic-based forecasts.

Tian et al. (2019) concluded that storm events with equally distributed spatial rainfall performed better in the WRF model, however storm events with a high intensity and short duration were difficult for the WRF models to manage. Without data assimilation, WRF-generated rainfall predictions frequently underestimated rainfall accumulation, particularly during intense events. They came to the conclusion that data assimilation can significantly enhance ensemble rainfall and flow forecasts.

Regimbeau et al. (2007) concluded that the flood peak is first anticipated with a one- or two-day inaccuracy and is underestimated; nonetheless, the information provided by the ensemble prediction can be useful for flood forecasting and water management organisations.

Thiemig et al. (2010) concluded that the potentials of a hydrological ensemble prediction system for flood forecasting employing EFAS-methodologies in conjunction with medium-range probabilistic meteorological predictions were examined for Africa, and seven out of eight examples indicated successful flood signals. In terms of timing and magnitude, there was a high level of precision.

Husain et al. (2018) used HEC-RAS software to predict floods at a number of gauge locations in Delhi. They concluded that the model could accurately predict flood for a particular gauge location while for other locations it overestimated the results.

Tran et al. (2020) concluded that physical hydrologic and hydraulic models with high fidelity should be used more frequently for real-time and ensemble flood forecasting.

Thiemig et al. (2015) concluded that the African Flood Forecasting System (AFFS) detected majority of the reported flood events correctly. With only a few ground

observations, the algorithm performed effectively and showed promise for future development as additional observational data were available. By supplying national and international relief organisations with timely medium-range flood forecast information, the system exhibited a significant potential to help to the reduction of flood-related losses in Africa.

2.1. OBJECTIVES OF THE PRESENT STUDY

- To prepare digital elevation maps (DEM), flow direction (FDR) and Flow accumulation maps (FAC) for Yamuna Ghat, Delhi using QGIS software.
- To develop a flood forecasting system for Delhi using Ensemble Framework for Flash Flood Forecasting.
- To compare the observed streamflow values with the simulated discharge values for a particular gauge point.
- To calculate bias, correlation coefficient and Nash-Sutcliffe Coefficient (NSCE) and check for the suitability of the model.

CHAPTER 3

METHODOLOGY

1. QGIS (Quantum – GIS)

It's a GNU General Public License-licensed open source geographic information system (GIS) that's easy to use. It prepares maps similar to Adobe Photoshop editing images. Maps are prepared in it from scratch, or from imported data. Even maps can be modified and existing maps may be added to the software. Each imported map or map feature is a “layer” in this software. Layers may be formed from point locations, background images, polygons such as country borders or more complex type of vector data like WMS maps or ESRI shape files. QGIS can only manipulate maps and can’t create new data.

1.1. TauDEM ALGORITHM PROVIDER

It's a collection of Digital Elevation Model (DEM) tools for extracting and analysing hydrologic data from topography represented by the DEM. It was created by Utah State University (USU) for watershed delineation and hydrologic digital elevation model analysis. It's a collection of standalone command-line executable applications for Windows, as well as source code for building and running on other platforms.

2. PRECIPITATION AND POTENTIAL EVAPO-TRANSPIRATION DATA USED FOR THE STUDY

2.1. PRECIPITATION DATA

Scientists from the USGS and the CHC have been developing strategies for making rainfall maps for locations where surface data is scarce since 1999. Flood early warning relies heavily on estimating rainfall variance in location and time. The precipitation grids in more rural locations, where there are fewer rain gauge stations, may not be accurate. CHIRPS was developed in collaboration with the United States Geological Survey's Earth Resources Observation and Science (EROS) Center to provide full, accurate, and up-

to-date data sets for a variety of early warning goals such as trend analysis and seasonal drought monitoring.

CHIRPS (Climate Hazards Group InfraRed Precipitation with Station Data) is a quasi-global rainfall data collection that spans 35 years. It runs from 500S to 500N (longitudes) and covers the years 1981 to the present. It also uses in-house climatology, CHPclim, 0.050 resolution satellite imagery, and in situ data to construct gridded rainfall time series that may be used for trend analysis and seasonal drought monitoring.

2.2. POTENTIAL EVAPOTRANSPIRATION (PET) DATA

Climate parameter data derived from Global Data Assimilation System (GDAS) analytical fields are used to produce the FEWSNET daily global potential evapotranspiration (PET) data. The National Oceanic and Atmospheric Administration generates this data every 6 hours (NOAA). Air temperature, atmospheric pressure, wind speed, relative humidity, and sun radiation are among the study's inputs. Penman-Monteith equations are used to determine the daily values.

3. CALIBRATION OF PARAMETERS IN EF5

Calibration is the process of adjusting model parameters so that model accurately simulates streamflow compared to the observed streamflow. After adjusting each parameter there are changes in the evaluation indices including bias, correlation coefficient and NSCE. Manual calibration is a time consuming process requiring active involvement. Automatic calibration solves this problem by searching the available parameter space using a single objective function and the hydrological model.

4. METHODOLOGY

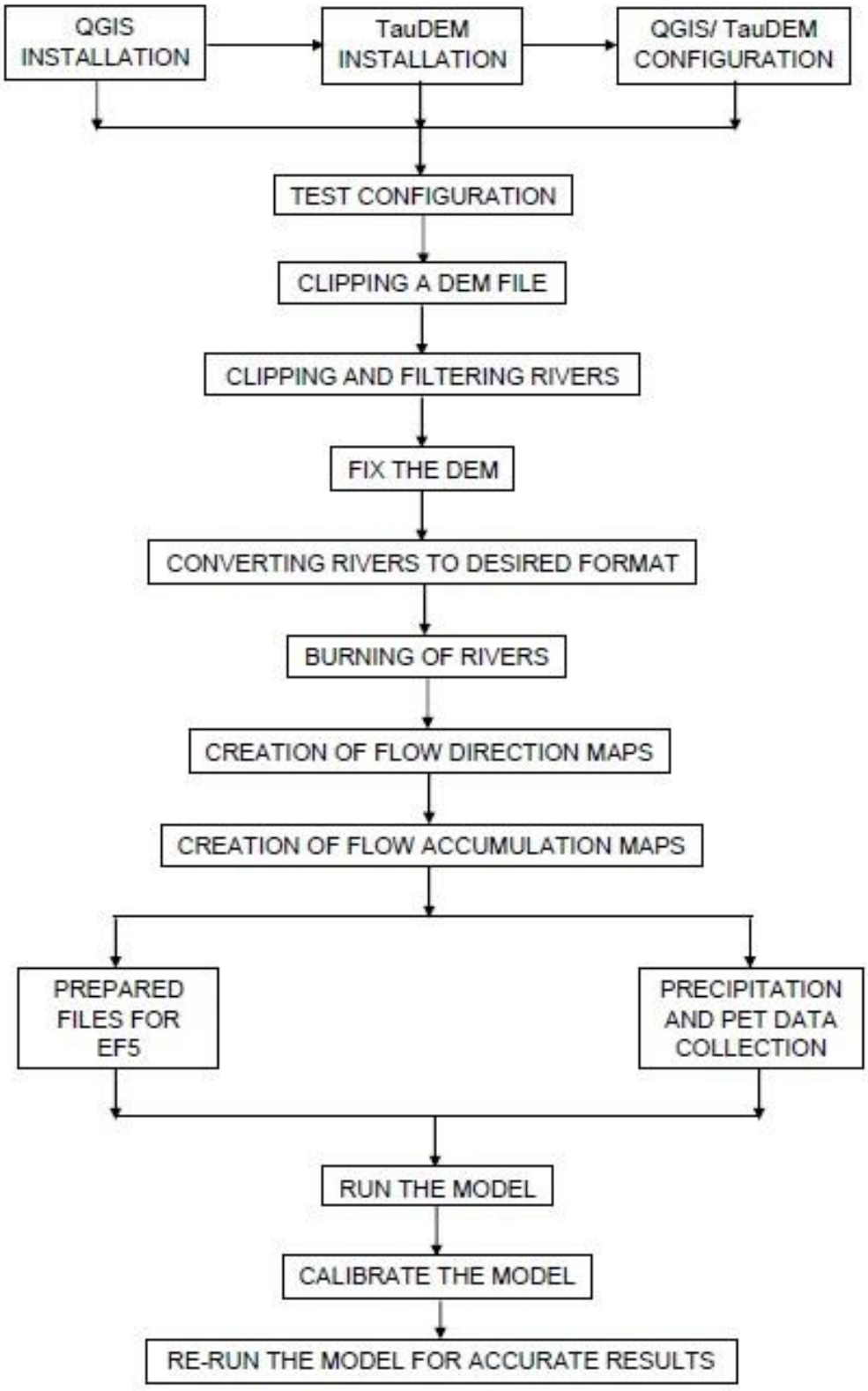

Figure 18: The EF5/SAC-SMA water balance component has a schematic depicting the flow of processes, inputs, and outputs.

5. STEPS FOLLOWED

5.1. INSTALLATION OF QGIS SOFTWARE

- To begin the project, one has to install QGIS software on the system.
- Selected the QGIS-OSGeo4W-2.6.1-1-Setup-x86_64.exe extension file.
- A popup window appeared on the screen.

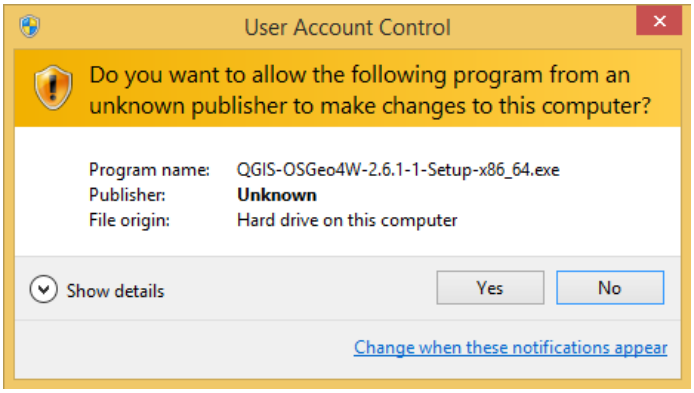

Figure 19: Popup menu during QGIS installation

- Answered “Yes” to continue with the installation of the QGIS software.
- A popup again appears on the screen “Welcome to the QGIS Brighton (2.6.1) setup Wizard”.

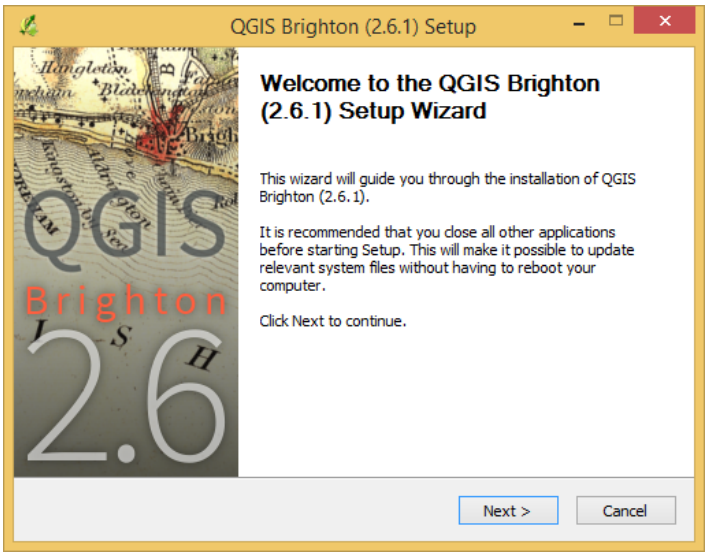

Figure 20: QGIS Setup Wizard

- Clicked “Next”. Agreed to the licence terms – “I Agree”.

- Chose the install location of the software – “C:\Program Files\QGIS Brighton” is fine; then clicked “Next”.

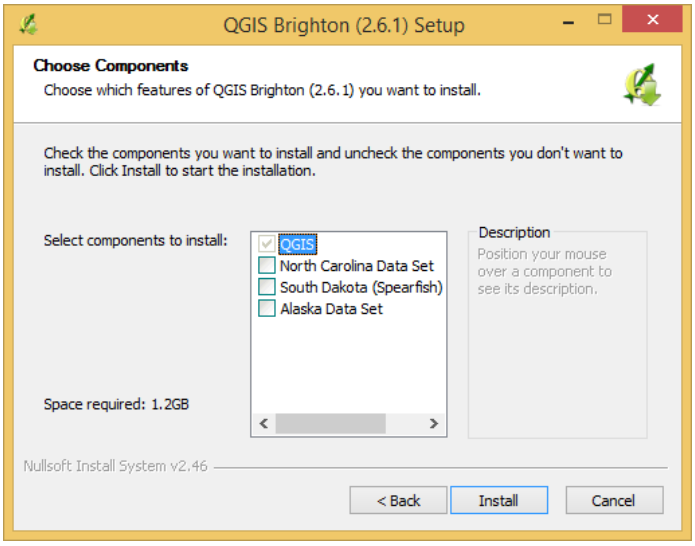

Figure 21: Options in QGIS Setup Wizard

- In the next window, from “Choose Components”, only installed “QGIS” and then clicked “Install”.

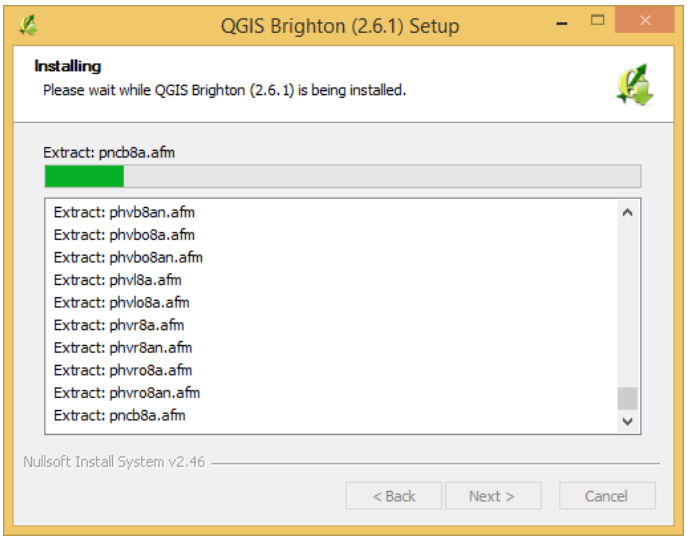

Figure 22: QGIS Setup Wizard Installation

- The process took 2-3 minutes to finish; then clicked “Finish”.
- The QGIS Desktop 2.6.1 application appeared on the desktop.
- Then I opened the QGIS application.

- In the “Processing menu” selected “Toolbox” and a new window pane appeared on the right side of QGIS.

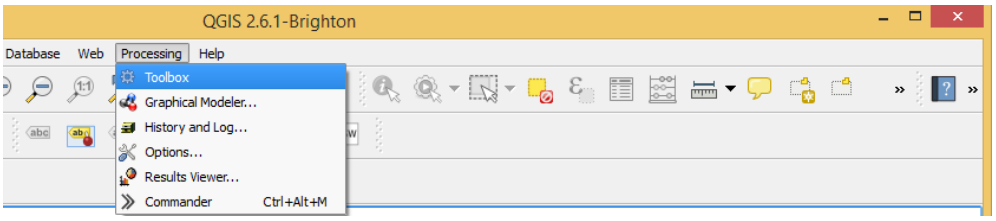

Figure 23: Processing Menu Options

- At the bottom of the “Processing Toolbox”, I selected “Advanced Interface”.

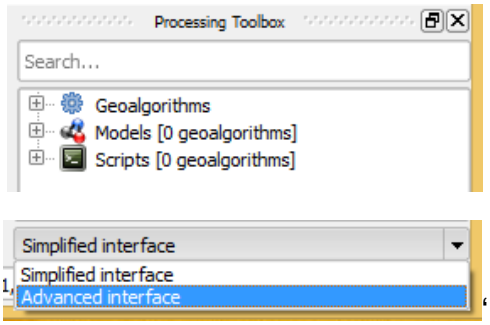

Figure 24: Processing Toolbox Options

- In the “Processing” menu selected “Options..”. Navigated to Providers – TauDEM (Hydrological Analysis) and checked “Activate”.

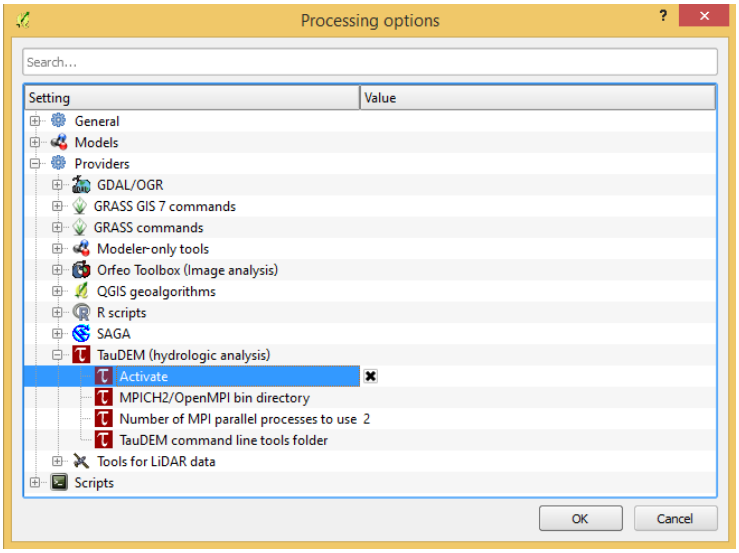

Figure 25: TauDEM activation in Processing Options

5.2. TauDEM INSTALLATION

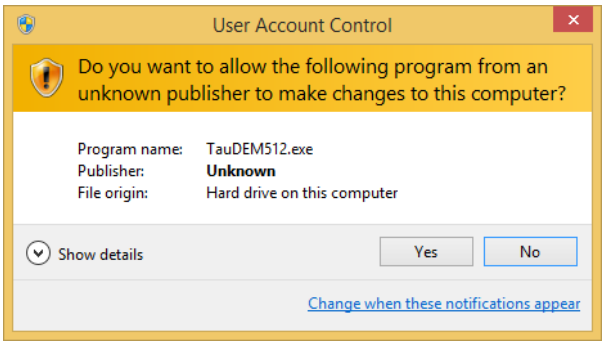

Figure 26: TauDEM Popup Menu

- Then I installed TauDEM. Open TauDEM512.exe extension file.
- Answered “Yes” to the UAC prompt.

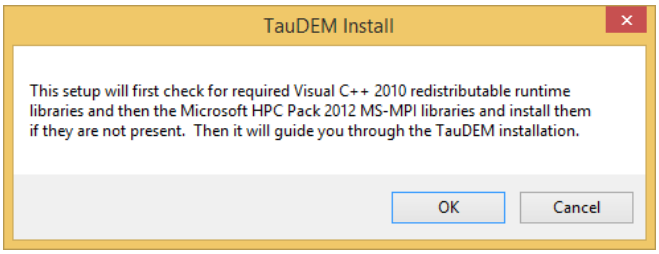

Figure 26: TauDEM Installation Wizard

- Selected “OK” at TauDEM install.

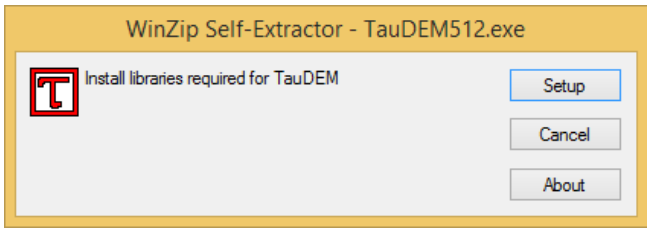

Figure 27: TauDEM Installation

- Selected “Setup” and then TauDEM began the Microsoft Visual C++ 2010 x86 installation.
- Clicked “Setup” and then accepted the licence terms.
- Clicked “Install” and then “Finish”.
- The Microsoft HPC Pack 2012 installation will then appear on the screen

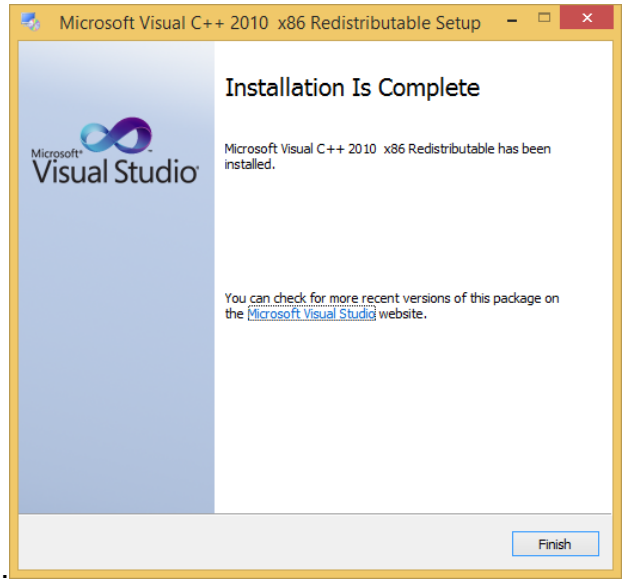

Figure 28: Intimation for TauDEM Installation Completion

- Clicked “Next” and then accepted the licence terms. Clicked “Install”.

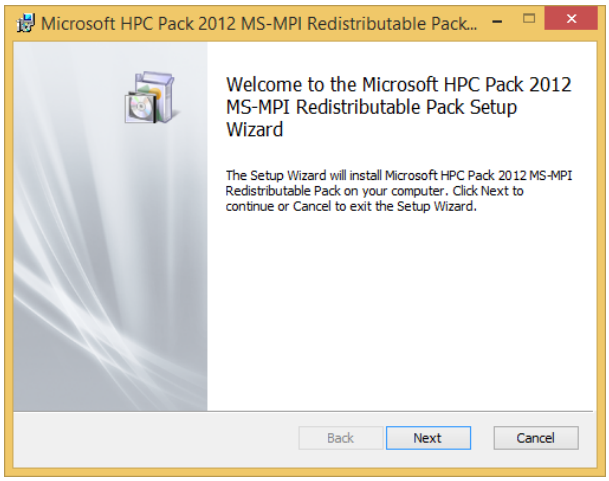

Figure 29: Microsoft HPC Pack Installation

- Then I downloaded and install .NET Framework version 3.5.

5.3. QGIS/ TauDEM CONFIGURATION

- In the QGIS software, selected “Options..”, from the “Processing” menu.
- Navigated to “Providers” and TauDEM (Hydrologic analysis)”.
- Typed “C:\Program Files\Microsoft HPC Pack 2012\Bin” next to “MPICH2/OpenMPI bin directory”.

- Typed “C:\Program Files\TauDEM\TauDEM5Exe” next to “TauDEM command line tools folder”.
- Made sure that QGIS saved that setting by clicking somewhere else inside the “Processing options” dialog.
- Clicked “OK”.

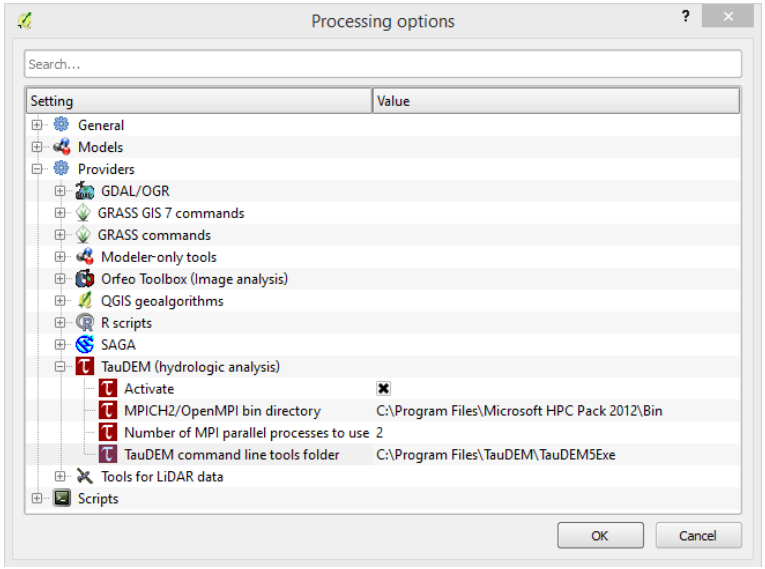

Figure 30: QGIS/ TauDEM Configuration

5.4. TEST CONFIGURATION

- Navigated to QGIS’s “Layers” menu, “Add Layer” and “Add Raster Layer..”.

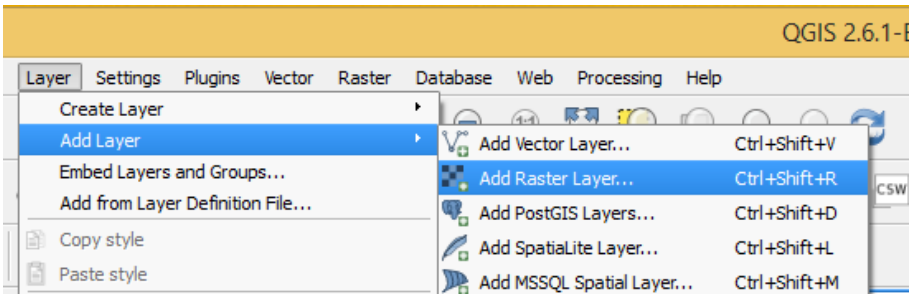

Figure 31: Opening of Raster Layer in QGIS Window

- In the dialog box, went to “\EF5_training\data\HydroSHEDS” and opened “test_dem.tif”.

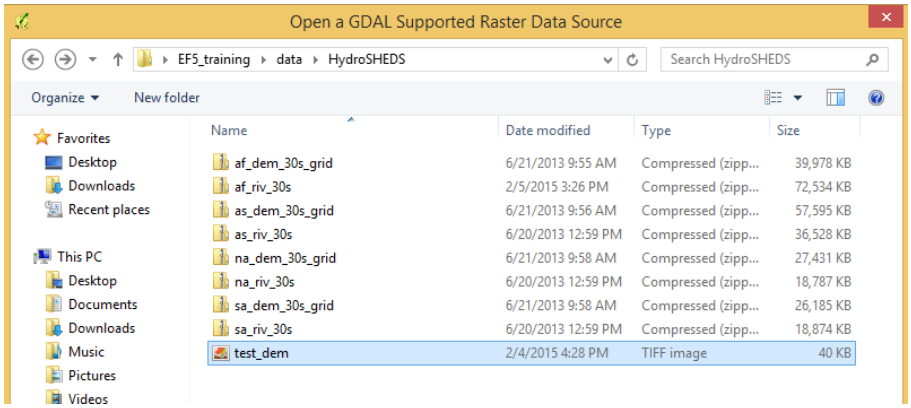

Figure 32: Opening of Raster Layer in QGIS Window

- In the “Processing toolbox”, searched for “Pit Remove” and double clicked.

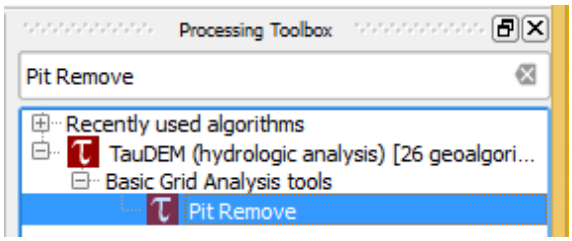

Figure 33: Checking for Pit Remove Function

- In the “Pit Remove” dialog box, selected “test_dem” as my “Elevation Grid” and for the “Pit Removed Elevation Grid” clicked “Save to fi le…”.

Figure 34: Option to Save Pit Removed Elevation Grid

- Saved the grid to “\EF5_training\examples\colombia\basic\dem.tif”.

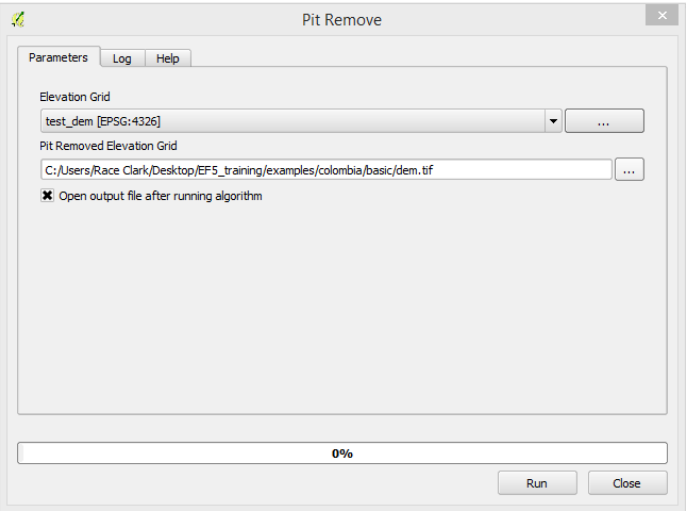

Figure 35: Saving the new file running pit remove function

- Now clicked “Run”.
- In the centre window of QGIS, there should be two maps: “test_dem” and “Pit Removed Elevation Grid”.
- If some error was displayed while running Pit Remove, something must have gone wrong in the installation process.
- Checked the file paths in the “Processing” menu “Options….” dialog.

5.5. CLIPPING A DEM

In GIS, clipping implies that the borders of the second polygon are forced on the first polygon. The rest of the space is discarded and no longer belongs to the initial polygon feature. The new data for the GIS file is the trimmed data. It is a significant function of GIS since it produced a research area or a specific region of interest. When working with GIS, it is critical to focus on a specific subject area of interest. Without affecting the main facts, the individual can remove the extraneous geographical information.

- Created a new folder on the desktop and named it Delhi.
- In “\EF5_training\data\HydroSHEDS”, unzipped “as_dem_30s_grid.zip” to the new Delhi folder.
- Right clicked and clicked “Extract All….”. Repeated it for “as_riv_30s.zip”.

- After this step, I opened the QGIS Desktop 2.6.1 application and added Vector Layer.

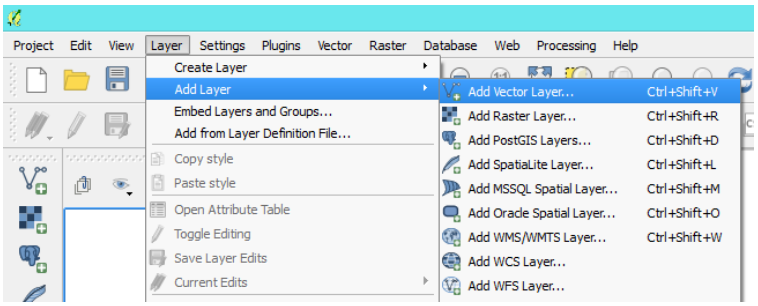

Figure 36: Adding Vector Layer to QGIS project

- At the prompt, navigated to Delhi folder and selected “as_riv_30s.shp”.
- Then I added a Raster Layer from the Delhi folder, selected as_dem_30s and then as_dem_30s again and then opened w001001.adf.
- The next step was to add my gauge location to the map (the Yamuna Ghat located on river Yamuna in Delhi). So I created a new shapefile layer.

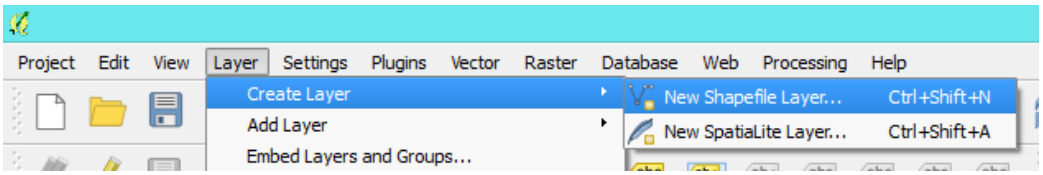

Figure 37: Creating a New Shape File

- Then I clicked “OK” and saved it as Delhi Bridge.shp within my Delhi folder.
- In the “layers” box at the left of the QGIS window, I dragged “as_riv_30s” up so its plotted over “w001001”.
- Then I used “Select features using an expression”. I typed UP_CELLS > 5000, then clicked “Select” and then “Close”.

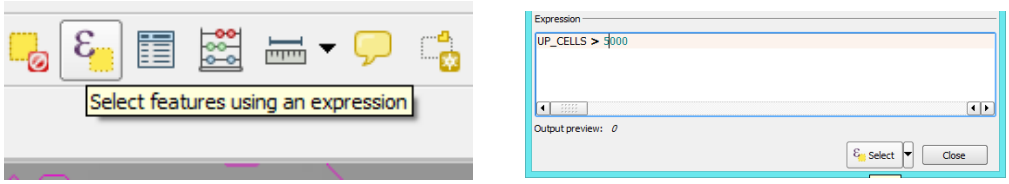

Figure 38: Working on Select Features using Expression

- Now I could see large rivers highlighted in a different colour.
- Turned on “Toggle Editing” and zoom in near the area of 77.24432339, 28.66400995 in the coordinate box at the bottom of the QGIS window.

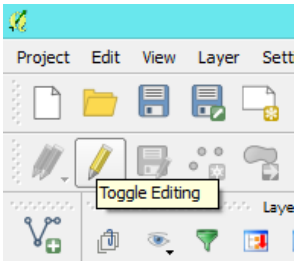

Figure 39: Turning on Toggle Editing to add a Gauge Point

- Selected “Add Feature” (the pencil icon next to “Delhi Bridge”).
- Then I clicked exactly at 77.24423229, 28.66400995 (it should be along one of the highlighted rivers). Type 1 in the “id” box.

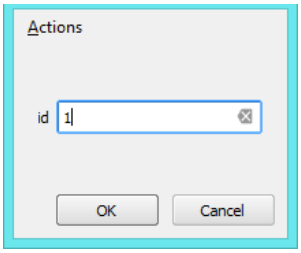

Figure 40: Naming of the new Gauge Point

- Now I turned off “Toggle editing” and saved changes to layer “Delhi Bridge” and zoomed out.
- Then next step was to identify the edges of the box covering the entire upstream area of our point. For that I selected the upper and lower latitudes and left and right longitudes for the analysis.
- Now I went to the “Raster” menu, “Projections” and clicked “Warp (Reproject)…”.

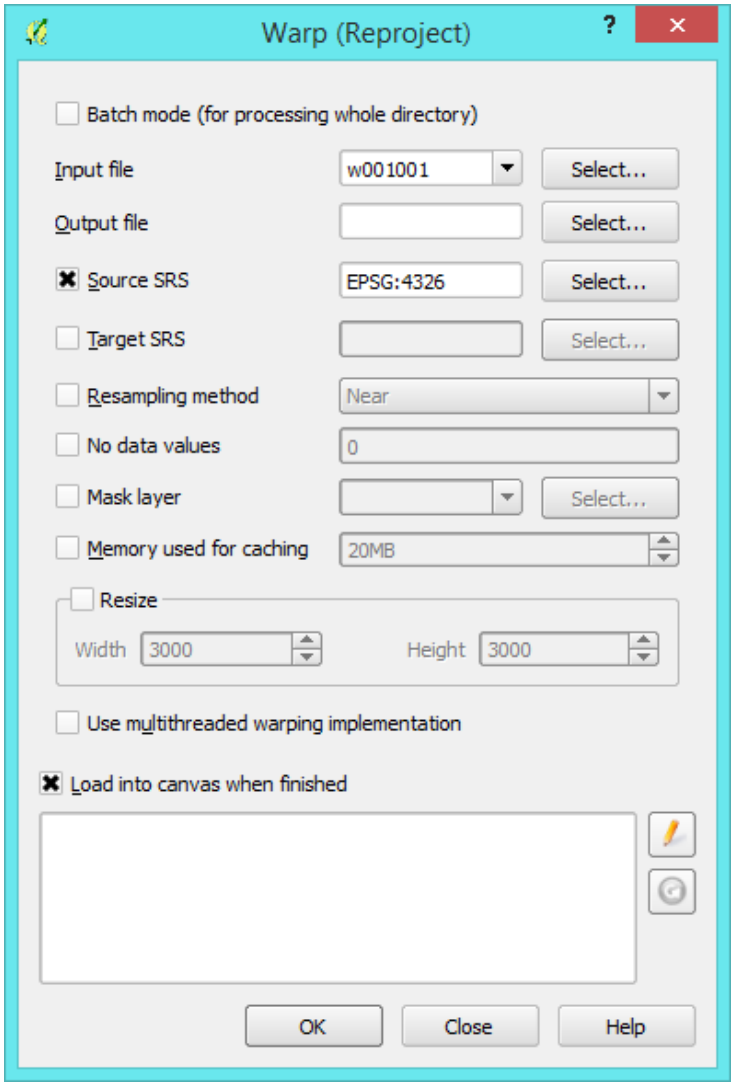

Figure 41: Working on Wrap (Reproject) function

- On this screen, clicked “Select…” by “Output file” and then saved to “Delhi” directory and used the name clipped_raster.tif.
- Then I checked “Resampling Method” and picked “Near”. Also I checked the no data values and typed “-32768”.
- Now I clicked on the pencil icon below “Load into canvas when finished”. After “-r near” typed “-te 32 76 28 79 –tr 0.125 0.125”.
- The output was as follows:

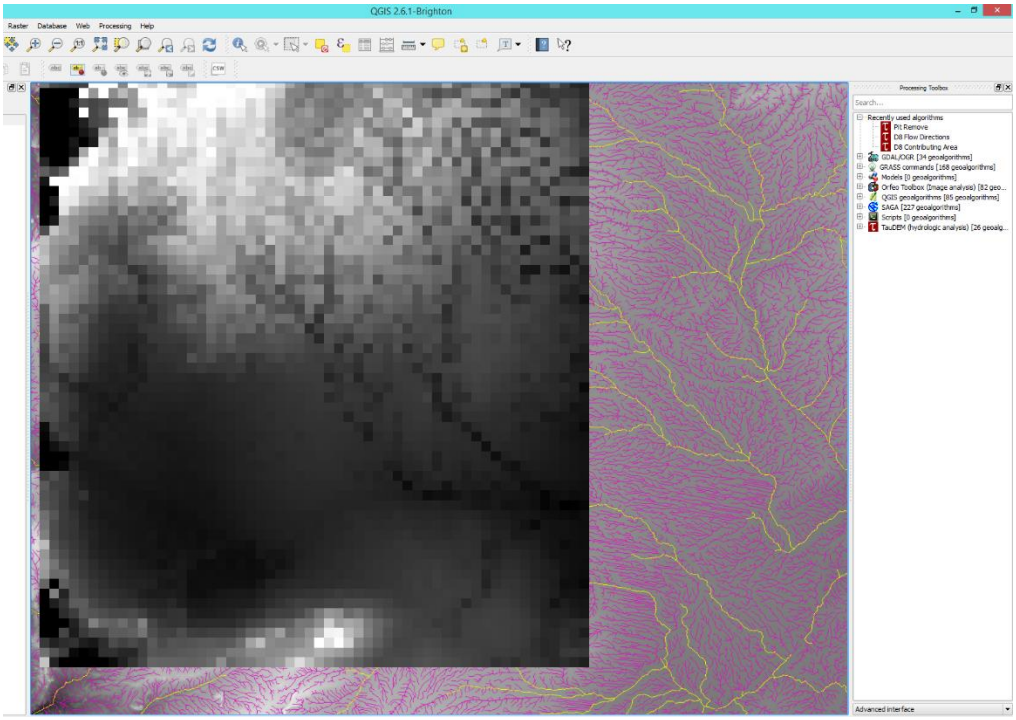

Figure 42: Preparation of DEM Files for Yamuna Basin

5.6. CLIPPING AND FILTERING RIVERS

- Now right clicked “af_riv_30s” and selected “Save As..”. Clicked Browse and then saved in the Delhi directory as “large_rivers.shp”.
- Checked “Save only selected features”. And then checked “Extent (current: user defined)”. Then, for north, south, east, and west, I typed the necessary numbers and clicked OK.

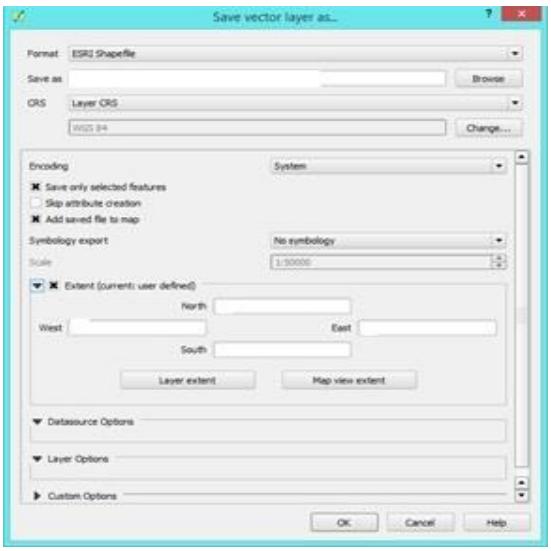

Figure 43: Clipping/ Filtering of Rivers

5.7. FIXING THE DEM

When we modify the DEM resolution, we tend to break things from the perspective of the model. We make drains or pits that were not present in the original data. To get rid of the pits, we convert our DEM file to the rectified version.

- In “Processing Toolbox”, selected “Pit Remove” from “Recently used algorithms”.
- Picked “clipped_raster” in the elevation grid drop down box and for “Pit Removed Elevation Grid” clicked the … and “Save to File”. Then I selected the appropriate location and named it “corrected_dem.tif”.
- Then I clicked “run” and when the process completed we have a new “Pit Removed Elevation Grid” in the “Layers” panel.

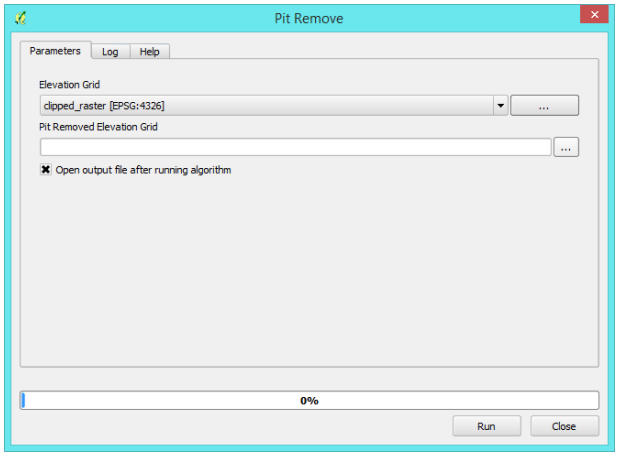

Figure 44: Fixing the DEM

5.8. CONVERTING RIVERS

I'll burn the rivers into the corrected DEM as part of this procedure to ensure that the model knows where the streams are.

- Went to “Raster” menu, “Conversion” and “Rasterize (Vector to Raster)…”.
- Selected “large_rivers” as the input file and “rasterized_rivers.tif” as the output file. Clicked OK on the popup warning.

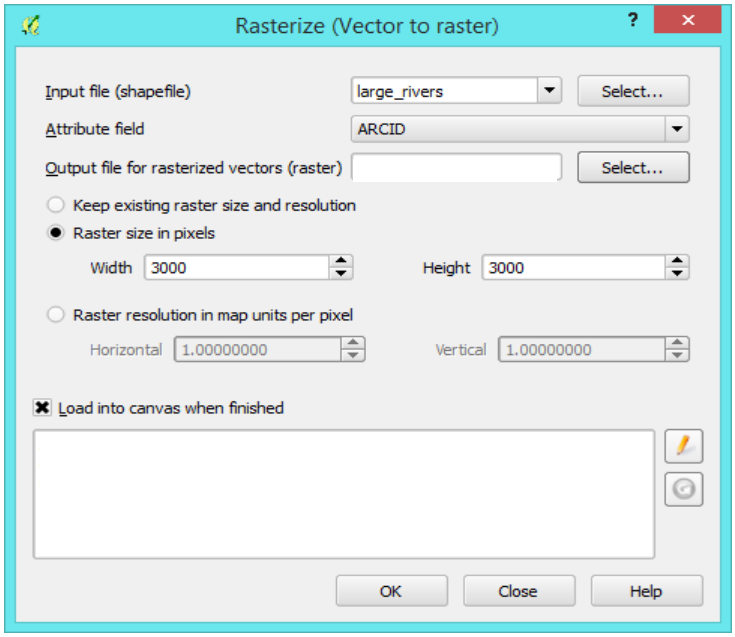

Figure 45: Converting Rivers to Desired Format

- Clicked the pencil icon near the bottom and in the text box deleted –a ARCID –ts 3000 3000 and replaced it with –burn -10 –te 32 76 28 79 –tr 0.125 0.125. Clicked “OK” “OK” and then “Close”.

5.9. BURNING RIVERS

The process by which we tend to reduce the pixels of each cell of the river is termed as burning the rivers into the DEM.

Figure 46: Burning of Rivers

- Now I added the rivers to the DEM.

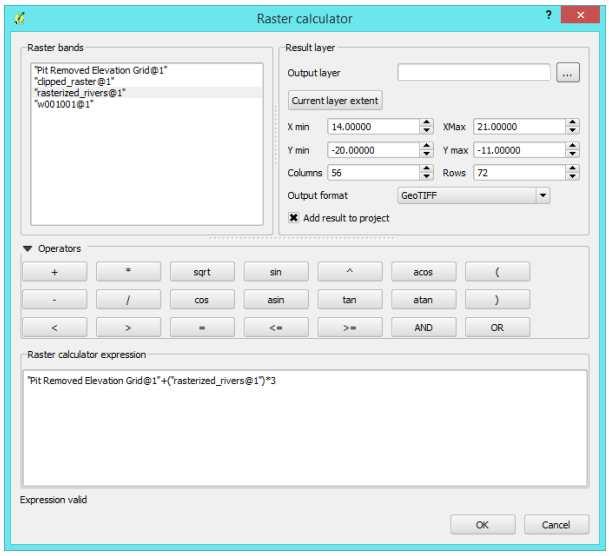

Figure 47: Raster Calculator for Burning of Rivers

- In the “Raster” menu selected “Raster Calculator”. In the “Output Layer” box, I saved the file as “burned_dem.tif”.
- In the “Raster bands” double clicked the “Pit Removed Elevation Grid”.
- At the bottom of the box, after Pit Removed Elevation Grid@1, typed +()*3 then moved the mouse between parentheses and double clicked “rasterized_rivers@1”.
- After clicking OK the output is as shown.

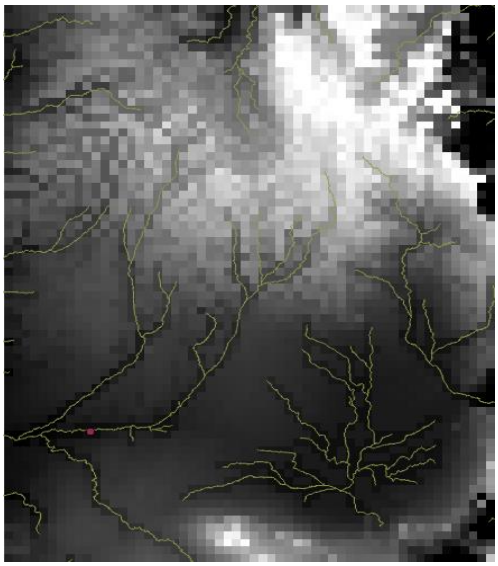

Figure 48: Burned Rivers

5.10. CREATING A FDR

A flow direction grid is a value-based grid that shows where the water is flowing.

- Saved the new pit removed elevation grid as dem.tif. This is the final DEM.
- In the “Processing Toolbox” opened “TauDEM (hydrologic analysis)” section, then “D8 Flow Directions”.

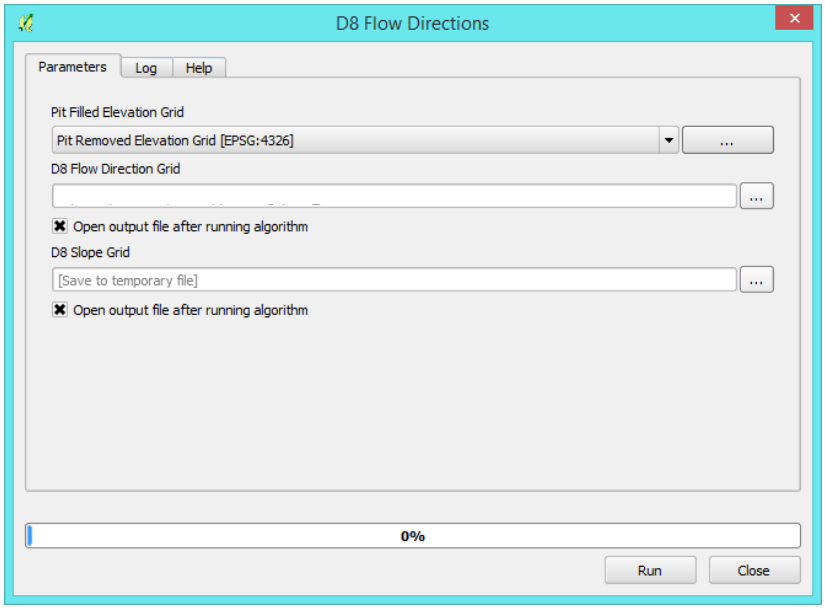

Figure 49: Creation of FDR

- Saved the new FDR as “flow_dir.tif”.

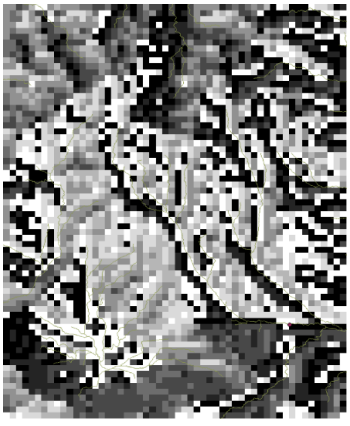

Figure 50: Created FDR

- I will now convert the file into format EF5 can read. In “Raster” menu, selected “Conversion” and then “Translate (Convert Format)…”.
- Saved the output file as “fdr.tif”.
- Then, after gdal translate, I clicked the pencil at the bottom and inserted –ot Float32 instead of –of GeoTIFF. Clicked “OK”, “OK” and “Close”.

5.11. CREATING A FAC

It's a grid of numbers that correlate to the number of cells that flow into each cell.

- In “Processing Toolbox”, go to TauDEM (hydrologic analysis) and then “Basic Grid Analysis tools” and then “D8 Contributing Area”.

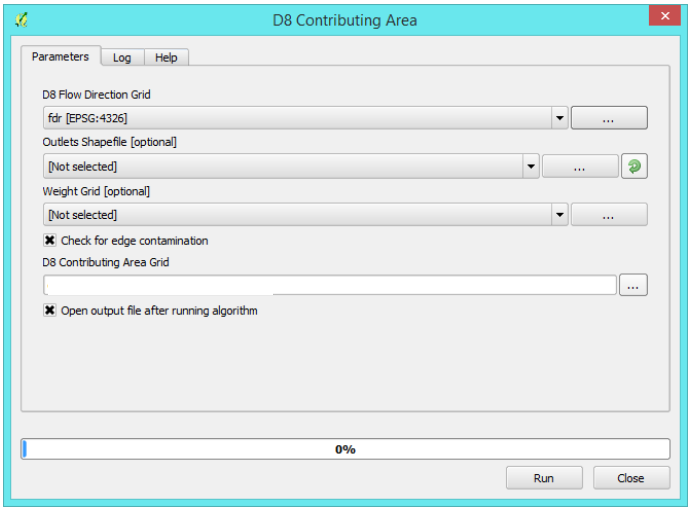

Figure 51: Creation of FAC

Figure 52: Created FAC

- Selected “fdr” for the “D8 Flow Direction Grid” and saved the “D8 Contributing Area Grid” as fac.tif. Clicked Run.

5.12. PREPARED FILES FOR EF5

- Exit QGIS after saving the QGIS project to the Delhi folder.
- Out of all the files in the Delhi folder, I copied dem.tif, fac.tif and fdr.tif to the Basic folder in Delhi.
- Also I added Delhi.csv file to obs folder which contains the observed discharge values for river Yamuna from 01-01-2001 to 31-12-2011.

5.13. PRECIPITATION AND PET DATA

- Downloaded the global potential evapotranspiration data from FEWS global flood forecasting website and copied it to pet folder in Delhi.
- Downloaded daily CHIRPS rainfall data from 01-01-2001 to 31-12-2011 and copied it to precip folder in Delhi.
- Then I opened the control file and checked the parameters for precipitation and potential evapotranspiration and fixed it as per my data.

5.14. CALIBRATING THE MODEL

- In the control file, I prepared the gauge file as per the requirement.
- Also I calibrated the CrestparamSet and KWParamSet blocks in the control file as per my model requirement.
- Then I in my Delhi folder, I created a new text document and named it RunEF5.txt. In that text file I typed EF5.exe and in next line Pause.
- I saved that file as RunEF5.bat.
- Now our model is ready to be executed and the output will be available in the obs folder based on which a hydrograph will be generated and studied further.

5.15. CALCULATION OF MODEL EVALUATION INDICES

- After plotting the hydrograph, the next step will be to calculated various model evaluation indices.

5.15.1. Bias

- It is thought as a shift up or down in a hydrograph.
- The higher the original value, the greater the bias.
- It may be stationary or non – stationary.
- Also it is expressed as a percent. It is preferred to be close to value zero.

$$\text{Bias} = \left[\frac{\sum_{i=1}^{n} R_{sim,i} - \sum_{i=1}^{n} R_{obs,i}}{\sum_{i=1}^{n} R_{obs,i}} \right] \times 100 \qquad (25)$$

Where,

$\sum_{i=1}^{n} R_{sim,i}$ is the total of all streamflow simulation values

$\sum_{i=1}^{n} R_{obs,i}$ is the total of all streamflow measurements

5.15.2. Correlation Coefficient

- This metric assesses the consistency of the simulation and observation time series.
- It is rated on a scale of 0 to 1, with 1 being the most desirable and 0 being the least desirable.
- If the bias specifies how much the simulation is vertically displaced from the data, the correlation coefficient only

evaluates the general displacement between the two-time series.

$$CC = \frac{\sum_{i=1}^{n}\left(R_{obs,i} - \overline{R_{obs}}\right)\left(R_{sim,i} - \overline{R_{sim}}\right)}{\sqrt{\sum_{i=1}^{n}\left(R_{obs,i} - \overline{R_{obs}}\right)^2 \sum_{i=1}^{n}\left(R_{sim,i} - \overline{R_{sim}}\right)^2}} \quad (26)$$

5.15.3. Nash-Sutcliffe Coeffecient (NSCE)

- It exists on a scale from -∞ to 1.
- In a general sense, NSCE can be depicted on a hydrograph as the amount of space or distance between the simulation and the observation,

$$NSCE = 1 - \frac{\sum_{i=1}^{n}\left(R_{obs,i} - R_{sim,i}\right)^2}{\sum_{i=1}^{n}\left(R_{obs,i} - \overline{R_{obs}}\right)^2} \quad (27)$$

CHAPTER 4

RESULTS AND DISCUSSIONS

- After preparing the model parameter and running the model batch file, the model runs as follows:

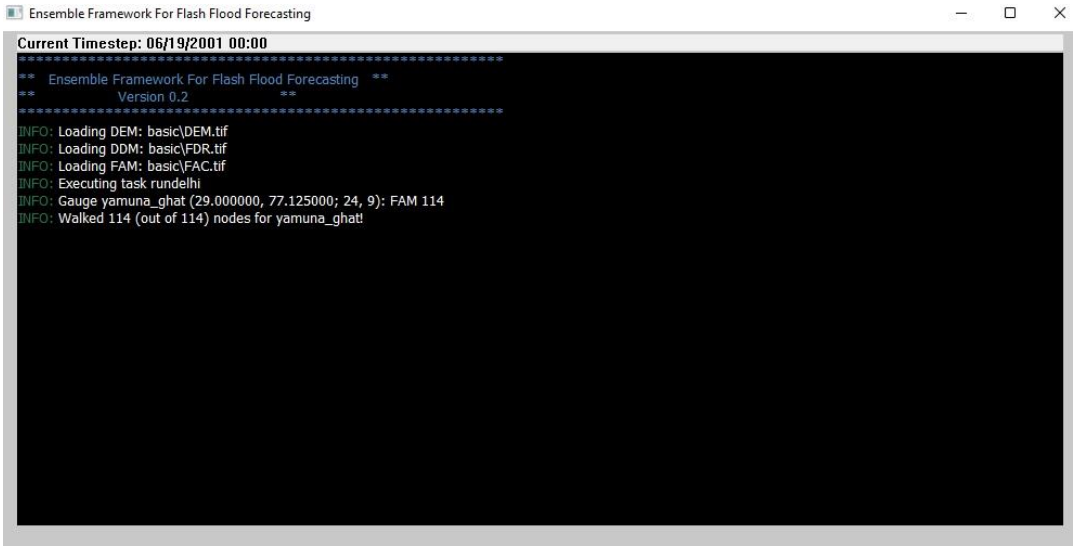

Figure 53: Running of Model Batch File

- After this process gets completed in the output folder of Delhi we obtain a .csv file named ts.yamuna_ghat.crest.csv.
- The output is displayed in the following format

678	11-08-2003 00:00	151.82	29.67	0	0.11	48.08	0	0
679	11-09-2003 00:00	145.85	29.31	0	0.11	47.49	0	0
680	11-10-2003 00:00	140.06	29.67	0	0.11	46.9	0	0
681	11-11-2003 00:00	134.53	28.26	0	0.11	46.32	0	0
682	11-12-2003 00:00	129.29	29.3	0	0.11	45.75	0	0
683	11/13/2003 00:00	124.33	31.76	0.01	0.11	45.35	0	0.0002
684	11/14/2003 00:00	119.89	33.55	0.11	0.11	46.41	0	0.0104
685	11/15/2003 00:00	116.22	31.27	0	0.11	45.89	0	0.0001
686	11/16/2003 00:00	113.28	31.27	0	0.11	45.34	0	0
687	11/17/2003 00:00	110.81	26.98	0.01	0.11	44.87	0	0.0004
688	11/18/2003 00:00	108.51	31.03	0	0.11	44.32	0	0
689	11/19/2003 00:00	106.12	32.38	0	0.11	43.78	0	0
690	11/20/2003 00:00	103.53	32.01	0	0.11	43.25	0	0
691	11/21/2003 00:00	100.72	33.64	0	0.11	42.72	0	0
692	11/22/2003 00:00	97.74	34.39	0	0.11	42.2	0	0
693	11/23/2003 00:00	94.68	34.39	0	0.11	41.69	0	0
694	11/24/2003 00:00	91.58	33.18	0	0.11	41.19	0	0

Figure 54: Part of .csv file depicting date, Stimulated discharge, Observed Discharge, Precipitation, PET, Soil Moisture, Fast Flow and Slow Flows

- Using the above data, a hydrograph is plotted. The plotted hydrograph is as follows:

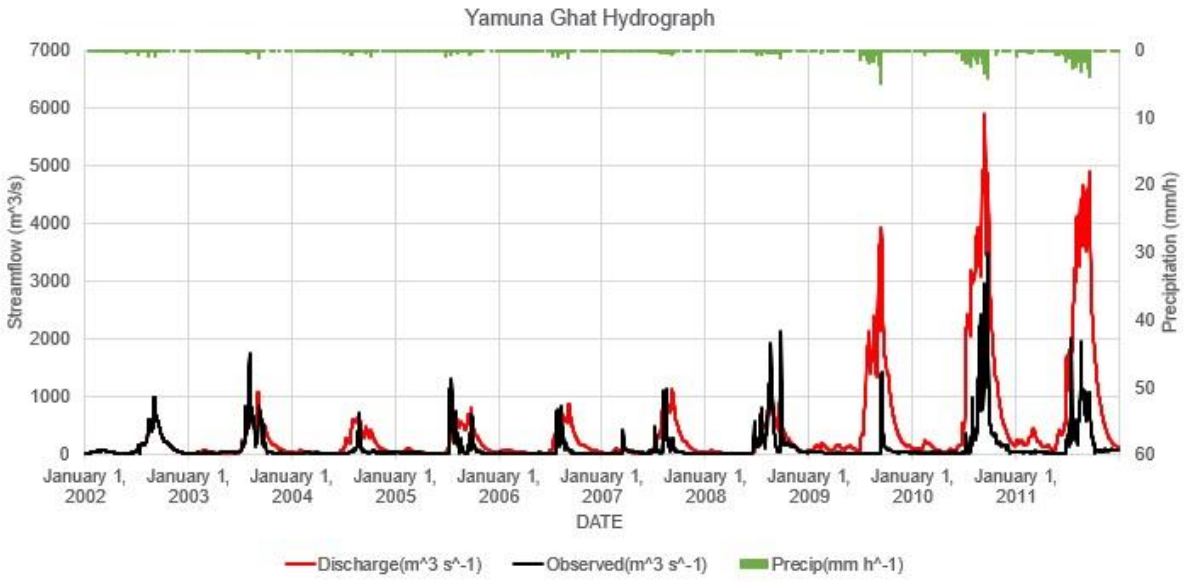

Figure 55: Output Hydrograph for the Simulated and Observed Streamflow

- When the simulated data is compared with the observed data, then it can be observed that there is a lot of discrepancy between the two datasets. It can be observed both numerically as well as through the plotted hydrograph. The model is over predicting the values of streamflow and therefore there is a need to calibrate the model so that the simulated values match with the observed values.
- Using these values may not be of use to hydraulic engineers because they might design the future hydraulic structures using the predicted values. This will consequently lead to overdesigning, make excess use of factor of safety for the structures and therefore the cost of these structures may increase tremendously.
- Also while working on future master planning of the city, the designers might have to leave more low lying area near the Yamuna river which is likely to be submerged due to the flooding conditions.
- Also the city's drainage system is designed as per the streamflow and water level of the river.
- Since many things are related to the streamflow and depth of water in a river, so accurate predictions of these results along with proper lead time will help authorities to execute work at a particular scale. So I will not use these uncalibrated results and work over it to get accurate values.

- In the control file the model parameters are readjusted and then the model is rerun. The new .csv file obtained after running the model is as follows:

678	08-11-2003 00:00	30.01	29.67	0	0.11	48.08	0	0
679	09-11-2003 00:00	29.32	29.31	0	0.11	47.49	0	0
680	10-11-2003 00:00	29.78	29.67	0	0.11	46.9	0	0
681	11-11-2003 00:00	28.27	28.26	0	0.11	46.32	0	0
682	12-11-2003 00:00	29.31	29.3	0	0.11	45.75	0	0
683	13-11-2003 00:00	31.77	31.76	0.01	0.11	45.35	0	0.0002
684	14-11-2003 00:00	33.56	33.55	0.11	0.11	46.41	0	0.0104
685	15-11-2003 00:00	31.26	31.27	0	0.11	45.89	0	0.0001
686	16-11-2003 00:00	31.28	31.27	0	0.11	45.34	0	0
687	17-11-2003 00:00	26.99	26.98	0.01	0.11	44.87	0	0.0004
688	18-11-2003 00:00	31.02	31.03	0	0.11	44.32	0	0
689	19-11-2003 00:00	32.39	32.38	0	0.11	43.78	0	0
690	20-11-2003 00:00	32.09	32.01	0	0.11	43.25	0	0
691	21-11-2003 00:00	33.65	33.64	0	0.11	42.72	0	0
692	22-11-2003 00:00	34.42	34.39	0	0.11	42.2	0	0
693	23-11-2003 00:00	34.4	34.39	0	0.11	41.69	0	0
694	24-11-2003 00:00	33.2	33.18	0	0.11	41.19	0	0

Figure 56: Part of the new .csv file depicting date, Stimulated discharge, Observed Discharge, Precipitation, PET, Soil Moisture, Fast Flow and Slow Flows

- Based on the new data, the hydrograph is plotted which will be as follows:

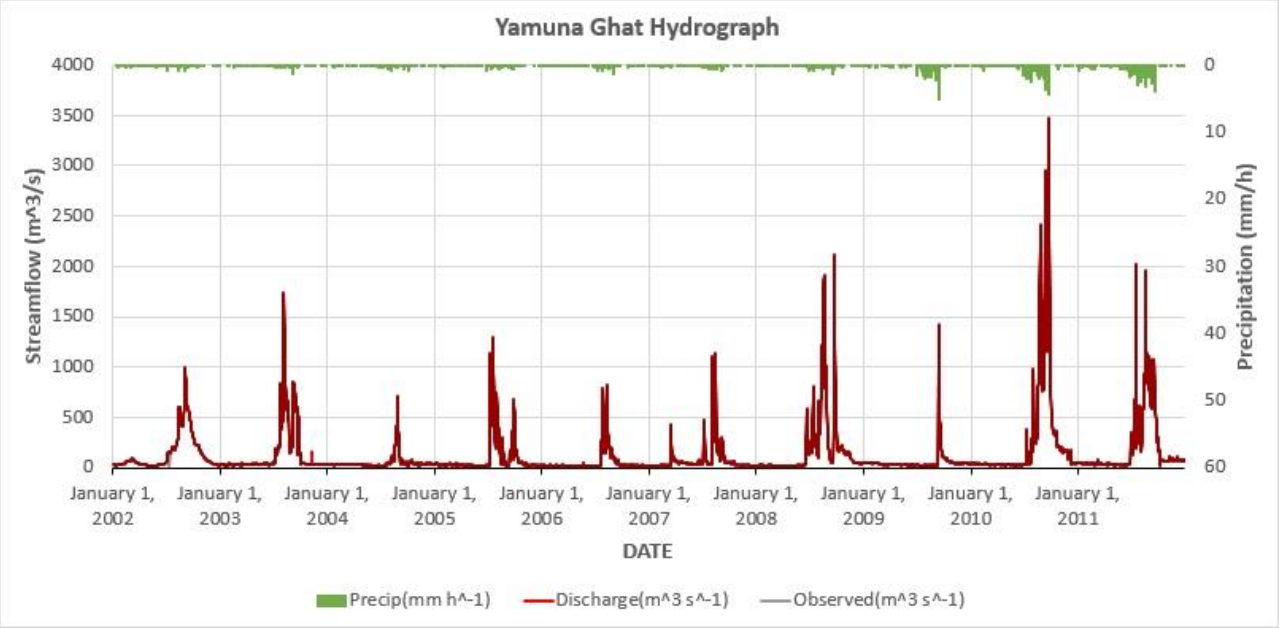

Figure 57: Calibrated Output Hydrograph for the Simulated and Observed Streamflow

- After plotting the hydrograph, the next step will be to calculated various model evaluation indices.
- The values of observed streamflow and simulated streamflow are nearly overlapping each other.

- After obtaining these results, I calculated various model evaluation as mentioned in the methodology above. The values of these indices were determined using the results obtained in the .csv file.
- The value of bias as obtained by the calculations comes out of be 4.78% which lies close to value 0.
- The value of correlation coefficient as calculated from the excel is 0.91 which lies to value 1 and is therefore an acceptable value.
- The value of nash-sutcliffe coefficient comes out to be 0.891 and this value also lies close to value 1.
- Based on these model evaluation indices, one can definitely observe that the model is working as per the acceptable requirements.
- This model is for a period of 2002 to 2011. One this model has been prepared then it can be used for future conditions as well based on the available datasets.
- Also for future conditions, India has developed models to predict ensemble precipitation values. But predicting rainfall is sufficient to determine the flooding conditions for a particular city.
- Using the ensemble predicted streamflow values is useful for determining if the river is capable of carrying that amount of flow or will overflow and cause flooding.
- Better planning of old cities as well as new cities can be done based on these values.
- Also it may help in building urban water resilience so that the city can withstand, absorb and recover in case of flooding with less possible damage.

CHAPTER 5
CONCLUSIONS

Based on the results and the calculation in the previous chapter, it can be concluded that the ensemble model for flood forecasting could be successfully calibrated since there is a negligible change between the observed discharge and the simulated discharge. The observed discharge values were provided as input to the model in .csv file format for a period of 01-01-2001 to 31-12-2011. Also a warm up time period was set up from 01-01-2001 to 31-12-2001 so that the model gets some estimates of the initial conditions. So in the output file we could get the simulated streamflow values, observed streamflow values, precipitation data, potential evapotranspiration data, soil moisture data, fast flow data (runoff) and slow flow data (percolation) in .csv file format.

All this data is available at a time interval which one has functioned in the control file. For the flood forecasting model, we only need the simulated streamflow data, observed streamflow data and precipitation data for the output time interval. Without working on the calibration, the output hydrograph was overestimating the streamflow conditions which may be similar to adding factor of safety to our design estimates. But using this overestimated design values may not be feasible for the hydraulic engineer in designing of the hydraulic structures as it may increase the cost of the project and the project may become economically unfeasible. But after working on automatic calibration of this model, a number of iterations were carried out the model, and based on the results obtained, the most suitable models parameters were used as input for the new control file. After running the model with these calibrated parameters, we can easily see from the hydrograph that the difference between the observed values and the calibrated values is negligible. Also the calculated model evaluation indices suggest that the chosen values are feasible for the model. Since I have setup the calibrated model for the Yamuna Ghat gauge point, it can easily be used for the future conditions if sufficient rainfall and potential evapotranspiration data is available for the future conditions as well. Using this model one can easily predict the streamflow in river Yamuna at Yamuna Ghat. Also one may add more gauge points on the Yamuna basin for analysis and based on the simulated values, future designing of hydraulic structures and master planning in Delhi may take place.

REFERENCES

[1] Allen, R.G., L. Pereira, D. Raes, and M. Smith, 1998. Crop Evapotranspiration, Food and Agriculture Organization of the United Nations, Rome, Italy. FAO publication 56. ISBN 92-5-104219-5. 290p.

[2] Haiyun Shi, Tiejian Li, Ronghua Liu, Ji Chen, Jiaye Li, Ang Zhang, Guangqian Wang, A service-oriented architecture for ensemble flood forecast from numerical weather prediction, Journal of Hydrology, Volume 527, 2015, Pages 933-942, ISSN 0022-1694, https://doi.org/10.1016/j.jhydrol.2015.05.056.

[3] Husain, Azhar & Sharif, Mohammed & Ahmad, Mohammed. (2018). Simulation of Floods in Delhi Segment of River Yamuna Using HEC-RAS. 162-168. 10.12691/ajwr-6-4-3.

[4] J.S. Nanditha, Vimal Mishra, On the need of ensemble flood forecast in India, Water Security, Volume 12, 2021, 100086, ISSN 2468-3124, https://doi.org/10.1016/j.wasec.2021.100086.

[5] Jiyang Tian, Jia Liu, Denghua Yan, Liuqian Ding, Chuanzhe Li, Ensemble flood forecasting based on a coupled atmospheric-hydrological modeling system with data assimilation, Atmospheric Research, Volume 224, 2019, Pages 127-137, ISSN 0169-8095, https://doi.org/10.1016/j.atmosres.2019.03.029.

[6] Konstantinos Bischiniotis, Bart van den Hurk, Ervin Zsoter, Erin Coughlan de Perez, Manolis Grillakis & Jeroen C. J. H. Aerts (2019) Evaluation of a global ensemble flood prediction system in Peru, Hydrological Sciences Journal, 64:10, 1171-1189, DOI: 10.1080/02626667.2019.1617868

[7] Li Liu, Chao Gao, Weidong Xuan, Yue-Ping Xu, Evaluation of medium-range ensemble flood forecasting based on calibration strategies and ensemble methods in Lanjiang Basin, Southeast China, Journal of Hydrology, Volume 554, 2017, Pages 233-250, ISSN 0022-1694, https://doi.org/10.1016/j.jhydrol.2017.08.032.

[8] Mukesh Kumar Tiwari, Chandranath Chatterjee, Uncertainty assessment and ensemble flood forecasting using bootstrap based artificial neural networks (BANNs), Journal of Hydrology, Volume 382, Issues 1–4, 2010, Pages 20-33, ISSN 0022-1694, https://doi.org/10.1016/j.jhydrol.2009.12.013.

[9] Sanjay Kumar, Report on Impact of Floods on Delhi (2017), School of Planning and Architecture, New Delhi.

[10] Shuttleworth, W.J., 1992. Evaporation. In D. Maidment, Handbook of Hydrology. McGraw-Hill.

[11] Smith, M. 1992. Expert consultation on the revision of FAO methodologies for crop water requirements. FAO, Rome, Italy. 60pp.

[12] Thiemig, V., Bisselink, B., Pappenberger, F., and Thielen, J.: A pan-African medium-range ensemble flood forecast system, Hydrol. Earth Syst. Sci., 19, 3365–3385, https://doi.org/10.5194/hess-19-3365-2015, 2015.

[13] Thiemig, V., Pappenberger, F., Thielen, J., Gadain, H., de Roo, A., Bodis, K., Del Medico, M. and Muthusi, F. (2010), Ensemble flood forecasting in Africa: a feasibility study in the Juba–Shabelle river basin. Atmosph. Sci. Lett., 11: 123-131. https://doi.org/10.1002/asl.266

[14] Tomar P, Singh SK, Kanga S, Meraj G, Kranjčić N, Đurin B, Pattanaik A. GIS-Based Urban Flood Risk Assessment and Management—A Case Study of Delhi National Capital Territory (NCT), India. Sustainability. 2021; 13(22):12850. https://doi.org/10.3390/su132212850

[15] Tran, V. N., Dwelle, M. C., Sargsyan, K., Ivanov, V. Y., & Kim, J. (2020). A novel modeling framework for computationally efficient and accurate real-time ensemble flood forecasting with uncertainty quantification. Water Resources Research, 56, e2019WR025727. https://doi.org/10.1029/2019WR025727

[16] Wu, Wenyan & Emerton, Rebecca & Duan, Qingyun & Wood, Andrew & Wetterhall, Fredrik & Robertson, David. (2020). Ensemble flood forecasting: Current status and future opportunities. Wiley Interdisciplinary Reviews: Water. 7. e1432. 10.1002/wat2.1432.

turnitin

Similarity Report ID: oid:27535:17883720

PAPER NAME
Thesis.pdf

AUTHOR
Varun

WORD COUNT
12425 Words

CHARACTER COUNT
64803 Characters

PAGE COUNT
73 Pages

FILE SIZE
3.6MB

SUBMISSION DATE
May 30, 2022 10:54 AM GMT+5:30

REPORT DATE
May 30, 2022 10:56 AM GMT+5:30

31/5/22

18% Overall Similarity

The combined total of all matches, including overlapping sources, for each database.

- 16% Internet database
- 8% Publications database
- Crossref database
- Crossref Posted Content database
- 5% Submitted Works database

Excluded from Similarity Report

- Bibliographic material
- Quoted material
- Small Matches (Less then 12 words)

Varun 2K20/HFE/07

Summary